



UNIVERSITAT POLITÈCNICA DE CATALUNYA  
BARCELONATECH  
Escola d'Enginyeria de Barcelona Est

FINAL THESIS

**Biomedical Engineering Degree**

**ELECTROCHEMICAL CHARACTERIZATION OF HYBRID  
FLEXIBLE AND BIORESORBABLE HYDROGELS**



**Memory and Appendices**

**Author:** Sergi Ortiz Torres  
**Director:** Joan Torras Costa  
**Co-Director:** Jillian Tricia Gamboa Rivera  
**Call:** January 2023



## Resum

Actualment, el món de l'enginyeria biomèdica aposta molt per la branca de l'enginyeria de teixits, no tant perquè ha estat poc estudiada sinó també per l'ampli ventall de possibilitats que ens pot oferir. En un esforç per desenvolupar aquesta branca, el grup de recerca IMEM (Innovació en Materials i Enginyeria Molecular) de la Universitat Politècnica de Catalunya pretén aplicar aquests coneixements al desenvolupament de polímers conductors biodegradables i flexibles per obtenir sensors flexibles, biocompatibles i bioresorbibles.

Els elèctrodes dels sensors de corrent estan fets majoritàriament de materials metàl·lics que, tot i que són adequats per les seves propietats conductores, els metalls no tenen propietats físiques semblants a les dels teixits vius d'un organisme. Aquesta és una de les raons per les quals aquest projecte se centra en el desenvolupament d'un elèctrode basat en hidrogel per utilitzar-lo en un sensor implantable.

Aquest treball de fi de grau es centra en dues parts fonamentals:

La primera part se centrarà a desenvolupar i fabricar els diferents hidrogels que es volen estudiar com a possibles candidats per utilitzar-los com a elèctrodes per a sensors implantables.

La segona part estarà destinada a caracteritzar aquests hidrogels desenvolupats. Aquesta part, que forma la majoria d'aquest projecte, pretén determinar la funcionalitat a llarg termini d'aquests hidrogels en un entorn in vitro. En aquesta caracterització es realitzaran assaigs per determinar les seves propietats de conductivitat i degradabilitat, així com l'estudi de les seves diferències d'estructura.

## Resumen

Actualmente, el mundo de la ingeniería biomédica está apostando fuerte por la rama de la ingeniería de tejidos, no tanto porque haya sido poco estudiada sino también por el amplio abanico de posibilidades que nos puede ofrecer. En un esfuerzo por desarrollar esta rama, el grupo de investigación IMEM (Innovación en Materiales e Ingeniería Molecular) de la Universitat Politècnica de Catalunya pretende aplicar este conocimiento al desarrollo de polímeros conductores biodegradables y flexibles para obtener sensores flexibles, biocompatibles y biorreabsorbibles.

Los electrodos de los sensores de corriente están hechos en su mayoría de materiales metálicos que, aunque adecuados por sus propiedades conductoras, los metales no tienen propiedades físicas muy similares a las de los tejidos vivos de un organismo. Esta es una de las razones por las que este proyecto se centra en el desarrollo de un electrodo a base de hidrogel para su uso en un sensor implantable.

Este trabajo de fin de grado se centra en dos partes fundamentales:

La primera parte se centrará en el desarrollo y la fabricación de varios hidrogeles destinados a ser estudiados como posibles candidatos para su uso como electrodos para sensores implantables.

La segunda parte estará encaminada a caracterizar estos hidrogeles desarrollados. Esta parte, que constituye la mayor parte de este proyecto, tiene como objetivo determinar la funcionalidad a largo plazo de estos hidrogeles en un entorno *in vitro*. En esta caracterización se realizarán ensayos para determinar sus propiedades conductivas y degradables, así como un estudio de sus diferencias estructurales.

## Abstract

Currently, the world of biomedical engineering is betting heavily on the branch of tissue engineering, not so much because it has been little studied but also because of the wide range of possibilities it can offer us. In an effort to develop this branch, the IMEM (Innovation in Materials and Molecular Engineering) research group of the Universitat Politècnica de Catalunya aims to apply this knowledge to the development of biodegradable and flexible conductive polymers to obtain flexible, biocompatible and bioresorbable sensors.

The electrodes of current sensors are mostly made of metallic materials which, although suitable for their conductive properties, metals do not have physical properties quite similar to those of the living tissues of an organism. This is one of the reasons why this project focuses on the development of an electrode based on hydrogel for use in an implantable sensor.

This final degree thesis project focuses on two fundamental parts:

The first part will focus on developing and fabricating the various hydrogels intended to be studied as possible candidates for use as electrodes for implantable sensors.

The second part will be aimed at characterizing these developed hydrogels. This part, which forms the majority of this project, aims to determine the long-term functionality of these hydrogels in an *in vitro* environment. In this characterization, tests will be carried out to determine its conductive and degradability properties as well as a study of their structure differences.

## Acknowledgments

First of all, I would like to thank the UPC IMEM research group for providing me with this opportunity to do the TFG with them. Thank you to each and every one of the doctoral and postdoc students for the amount of knowledge they have taught me and for the help received during the completion of the TFG.

Thanks to Dr. Joan Torras Costa for offering me the possibility to do this TFG, and for guiding me, helping me, and providing me with a lot of ideas throughout this TFG.

To the PhD student Jillian Gamoba Rivera for all the knowledge learned and the advice given for the completion of this work, as well as the patience and support she has shown in the moments when things did not turn out as we expected.

Finally, I would like to thank my family, without whom I would not be where I am and would not be the person I am today. For always being by my side, celebrating the happy days and supporting me in the darkest ones.

To all, thank you very much.

## Glossary

<b>CP</b>	Conductive Polymer
<b>CQD</b>	Carbon Quantum Dots
<b>CV</b>	Cyclic Voltammetry
<b>FIB</b>	Focused Ion Beam
<b>FTIR</b>	Fourier-transform infrared spectroscopy
<b>LEA</b>	Loss of Electroactivity
<b>Mw</b>	Molecular Weight (g/mole)
<b>PBS</b>	Phosphate-Buffered Saline
<b>PEDOT:PSS</b>	Poly(3,4-ethylenedioxythiophene) polystyrene sulfonate
<b>PVA</b>	Poly(vinyl alcohol)
<b>SC</b>	Specific Capacitance
<b>SEM</b>	Scanning Electron Microscopy
<b>TA</b>	Tannic Acid
<b>UV-VIS</b>	UV–visible spectrophotometry





# Índex

<b>RESUM</b>	<b>I</b>
<b>RESUMEN</b>	<b>II</b>
<b>ABSTRACT</b>	<b>III</b>
<b>ACKNOWLEDGMENTS</b>	<b>IV</b>
<b>GLOSSARY</b>	<b>V</b>
<b>1. PREFACE</b>	<b>15</b>
1.1. Motivation .....	15
1.2. Previous Requirements .....	15
1.3. Objectives of the project .....	15
<b>2. THEORETICAL FOUNDATIONS</b>	<b>16</b>
2.1. Polymers .....	16
2.1.1. Classification .....	16
2.1.2. Polymerization .....	18
2.2. Biodegradable Polymers .....	18
2.2.1. PVA .....	19
2.3. Conducting Polymers .....	20
2.3.1. Polymer Doping .....	21
2.3.2. PEDOT:PSS .....	22
2.4. Hydrogels .....	22
2.5. Additives .....	23
2.5.1. Carbon Quantum Dots .....	23
2.5.2. Tannic Acid .....	24
2.6. TECHNIQUES .....	25
2.6.1. Cyclic Voltammetry (CV) .....	25
2.6.2. SEM .....	26
2.6.3. RAMAN .....	27
2.6.4. FTIR .....	28
<b>3. EXPERIMENTAL METHOD</b>	<b>29</b>
3.1. Methodology and Materials .....	29
3.1.1. Carbon Quantum Dots .....	29
3.1.2. TA solution .....	29
3.1.3. Hydrogels .....	30



3.1.4.	PBS .....	31
<b>4.</b>	<b>HYDROGEL CHARACTERITZATION</b> .....	<b>32</b>
4.1.	CYCLIC VOLTAMMETRY .....	33
4.1.1.	Solid-State Cyclic Voltammetry .....	33
4.1.2.	Liquid-State Cyclic Voltammetry .....	34
4.2.	DEGRADATION .....	35
4.3.	CHARACTERIZATION TESTS .....	36
4.3.1.	Swelling Ratio .....	36
4.3.2.	SEM .....	36
4.3.3.	FTIR .....	37
4.3.4.	RAMAN .....	38
<b>5.</b>	<b>RESULTS AND DATA ANALYSIS</b> .....	<b>39</b>
5.1.	CYCLIC VOLTAMMETRY .....	39
5.1.1.	3rd CV Cycle of Hydrogels (8-Week test) .....	39
5.1.2.	TA and CQD solution CV .....	41
5.2.	Specific Capacitance (SC).....	45
5.2.1.	3rd Cycle Specific Capacitance (8 weeks test) .....	45
5.3.	Degradation and Swelling Ratio .....	47
5.3.1.	8 Week Degradation Test .....	47
5.3.2.	8 Week Swelling Test.....	49
5.4.	SEM .....	51
5.4.1.	Pore Size and Distribution .....	52
5.5.	FTIR .....	55
5.6.	RAMAN .....	57
5.7.	Final Data Analysis.....	59
<b>6.</b>	<b>ENVIRONMENTAL IMPACT ANALYSIS</b> .....	<b>62</b>
	<b>BUDGET AND ECONOMIC ANALYSIS</b> .....	<b>65</b>
	<b>CONCLUSIONS</b> .....	<b>68</b>
	<b>BIBLIOGRAPHY</b> .....	<b>70</b>
	<b>ANNEXES</b> .....	<b>75</b>
A1.	Cyclic Voltammetry .....	75
A2.	Degradation .....	76
A3.	Swelling Ratio .....	76

A4. SEM .....	77
A5. FTIR .....	78

## **Index of Figures**

Figure 1 Polymerization of styrene to form polystyrene [1]	16
Figure 2 Polymer arrangement types [3]	17
Figure 3 Polymer crystallinity types [3]	18
Figure 4 PVA chemical structure [8]	19
Figure 5 Freeze-Thawing method representation [7]	20
Figure 6 Representation of how doping work on CPs [13]	21
Figure 7 PEDOT:PSS chemical structure [15]	22
Figure 8 CQD applications scheme [20]	24
Figure 9 Tannic Acid chemical structure [23]	25
Figure 10 Example of a cyclic voltammogram [26]	26
Figure 11 PhenomXL Desktop SEM (left) and Neon40 Crossbeam (right) used to perform visual examination of the samples	27
Figure 12. Renishaw's inVia Qontor Raman microscope	27
Figure 13 Spectrophotometer FT/IR-4700 from Jasco Corporation	28
Figure 14. a) Autoclave used to heat CQD solution, b) CQD solution after 12h at 180 °C at the autoclave, c) CQD solution after solvent drying and redispersion in Milli Q water, d) CQD solution under UV light	29
Figure 15 Assembly used for PVA solution preparation	30
Figure 16 Hydrogel sample placed between ITO layers to perform CV	33
Figure 17 Assembly used for solid-state cyclic voltammetries	34

---

Figure 18 Assembly used to perform liquid-state cyclic voltammetries _____	34
Figure 19. Sample preparation and storage for the swelling and degradation tests (left) and a hydrogel A (PEDOT:PSS + TA) dry sample after lyophilization _____	35
Figure 20 Hydrogel A (PEDOT:PSS + TA) SEM image (10kV, 1500x) and further ImageJ pore analysis _____	37
Figure 21 FTIR of the PVA only hydrogel on Week 0 _____	38
Figure 22 3rd Cycle CV of all hybrid hydrogels of the 8 weeks test _____	39
Figure 23 Visual test of TA release in samples of all hydrogel types preserved in PBS and agitation for 1 week. From left to right: Hydrogels A (PEDOT:PSS + TA + CQD), B (TA + CQD), C (PEDOT:PSS + TA + CQD), D (PVA only), CQD only, TA only and PEDOT:PSS only _____	40
Figure 24 CV of 1.5% TA solution scanned at 50 mV/s using 0.5M KCl as supporting electrolyte. _____	42
Figure 25 CV of 1.5% CQD solution scanned at 50 mV/s using 0.5M KCl as supporting electrolyte. _____	43
Figure 26 CV of TA and CQD at different ratios scanned at 50 mV/s using 0.5M KCl as supporting electrolyte _____	44
Figure 27 8 weeks SC (cycle 3) test of all hybrid hydrogels _____	45
Figure 28 SC on cycle 3 vs cycle 50 of all hybrid hydrogels during 8 weeks _____	46
Figure 29 8 weeks degradation test of all hybrid hydrogels _____	47
Figure 30 8 weeks swelling ratio test of all hybrid hydrogels _____	49
Figure 31 Pore diameter size histograms of all hybrid hydrogels on week 0 (left) and week 4 (right) _____	53
Figure 32. Week 0 (left) and Week 4 (right) FTIR of all hybrid hydrogels _____	55
Figure 33 CQD + TA hydrogel fluorescence under UV light to test visually the presence of CQD. _____	56

---

Figure 34 Week 0 Raman spectrum of all hybrid hydrogel from 2700 $\text{cm}^{-1}$ to 3200 $\text{cm}^{-1}$ to observe the PVA peak	57
Figure 35 Raman spectrum from 800 to 1750 $\text{cm}^{-1}$ to show the PEDOT:PSS peaks at Week 0 (left) and Week 4 (right)	57
Figure 36 Single Component hydrogels CV compared with the PVA only	75
Figure 37 Day 7 degradation of single component hydrogels after 1 week test	76
Figure 38 1 Week Swelling ratio test of single component hydrogels	76
Figure 39 Visual comparison of single component hydrogels cross section	77
Figure 40 Single component hydrogels pore size histograms on week 0	77
Figure 41 FTIR spectrums of the single component hydrogels on week 0	78
Figure 42 Comparison of FTIR spectrums on Week 0 and Week 4 of all hybrid hydrogels	78

## Index of Tables

Table 1 Percentages of each additive used in every hybrid and single component hydrogel	30
Table 2 Total of samples testes per hydrogel and per test through the project	32
Table 3 SEM images of all hybrid hydrogels on week 0 and week 4 taken with a 3000x magnification and intensities between 5 and 15 kV	51
Table 4 Hybrid hydrogels mean pore diameter on weeks 0 and 4 with standard deviations	52
Table 5 Comparative table of Degradation, Swelling Ratio, SC and Pore Size of Week 0 samples	59
Table 6 Comparative table of Degradation, Swelling Ratio, SC and Pore Size values of Week 4 samples	59
Table 7 Power consumption during the project and the equivalent kg of CO <sub>2</sub> produced considering a production of 250g of CO <sub>2</sub> per kW/h	62
Table 8 Total cost of the reagents used in the project	65
Table 9 Cost of the working ours based on a mean Junior Biomedical Engineer salary of 21.500€ a year [48]	66
Table 10 Cost of project correction based on a mean Senior Engineer salary in Barcelona of 55.700€ a year [49]	66
Table 11 Total cost of the used equipment in the laboratory for the characterization. Prices are provided by the Barcelona Research Center in Multiscale Science and Engineering	66
Table 12 Cost of the laboratory equipment used to perform the test based on their lifespan and time of use	67





# 1. Preface

## 1.1. Motivation

During the course of the degree I have been able to see all the paths that biomedical engineering can provide me. Although not all of them have coincided with my preferences and intentions, some of them have awakened a curiosity that I wanted to explore further. This is where the motivation for this TFG comes from the need to apply the concepts of two of the subjects that have stood out the most in me, which are biomaterials and tissue engineering. Hence, when Dr. Joan Torras and PhD Jillian Gamboa presented their TFG proposal I found the ideal opportunity.

At the same time, my path in university life began in Chemical Engineering (although in the end it will end in Biomedical Engineering). This work combines many concepts from these two branches of engineering, and it is for this reason that this project was an exceptional opportunity to combine the concepts of the two areas.

## 1.2. Previous Requirements

For this project no previous requirements were needed as all protocols and tests were learned during the project.

## 1.3. Objectives of the project

In this project various objectives are pretended to be obtain at the end. As it was explained in the abstract the project is based on two parts, the hydrogel fabrication and the characterization. Hence, the objectives that this project intend to achieve are:

- Fabricate the different hybrid hydrogels with the desired additive concentrations.
- Determine the electroactive behaviors of the various hydrogels.
- Find the degradative and swelling trends as well as the maximum and minimum values over time.
- Determine the chemical structure and the presence of additives through different characterization techniques.
- Observe and determine the effect of additives in hydrogels properties.

## 2. Theoretical Foundations

An introduction of fundamental concepts is performed to better understand and explain the procedures used and results obtained in the project.

### 2.1. Polymers

Polymers have a wide range of characteristics, both physical and chemical, that they are an essential part of daily life. They can be found everywhere, from basic proteins for life to materials for construction, paints, medical applications, among others.

The word polymer comes from two Greek words, 'poly' that means many and 'meros' that means parts. Hence polymers, based on their most basic meaning, are structures formed by the repeated union of smaller units called monomers. According to their origin, polymers can be classified as synthetic or natural [1].

Polymers are formed through a process called polymerization in which the various monomers are joined through covalent bonds to create the final structure [1].

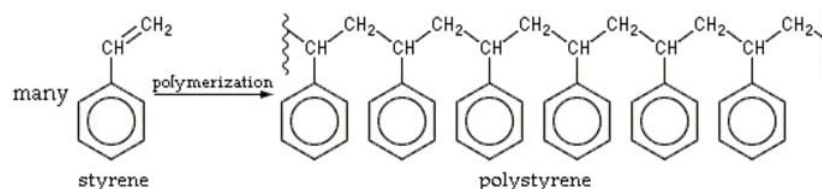


Figure 1 Polymerization of styrene to form polystyrene [1]

#### 2.1.1. Classification

Due to the great structural and functional complexity of polymers, a single classification cannot be made, but this can be divided according to various criteria such as nature, structure and functionality.

##### 2.1.1.1. Nature of the polymer

Polymers can be classified as natural or synthetic. Natural polymers are polymers found in nature. These include deoxyribonucleic acid or DNA, which hold the genetic makeup of all living creatures, and proteins and enzymes, which carry out many vital processes in the body. On the other hand, synthetic polymers are man-made polymers and we find fibers, plastics, paints, adhesives, etc [2].

### 2.1.1.2. Polymer Structure

Polymer complexity is due, in part, to the numerous possible arrangements of the monomers in the structure. Hence, polymers can also be classified according to their structure: linear, branched and crosslinked.

If these monomers are linked through two points (and only two points), the chain will be linear. On the other hand, if the monomers allow connections at various points in their structure, a branched chain is formed. Finally, when the various chains of the polymer join together, a crosslinked chain is formed [2].

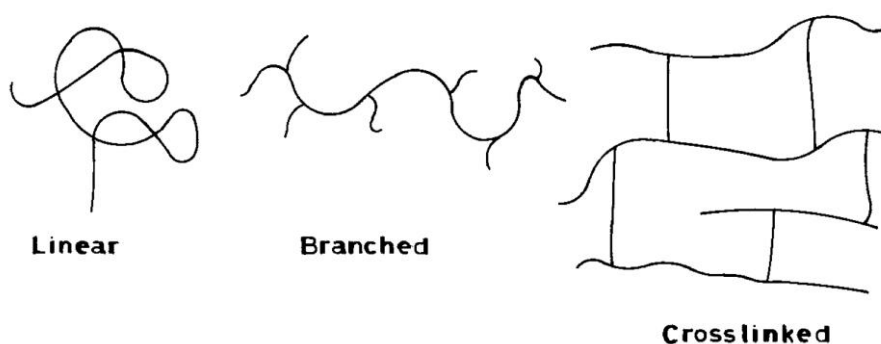


Figure 2 Polymer arrangement types [3]

### 2.1.1.3. Crystallinity

Polymers can also be classified according to its degree of crystallinity. When a molten polymer or polymer in solution is cooled, the polymer chains tend to group together to have the lowest possible potential energy, which is the most stable state. During this process, if the polymer chains are deposited in an orderly manner along the entire structure, a crystalline polymer is achieved. On the other hand, if these chains are deposited in a random arrangement, this results in an amorphous polymer [2].

Finally, materials can also contain both types of arrangements, thus obtaining a semi-crystalline polymer.

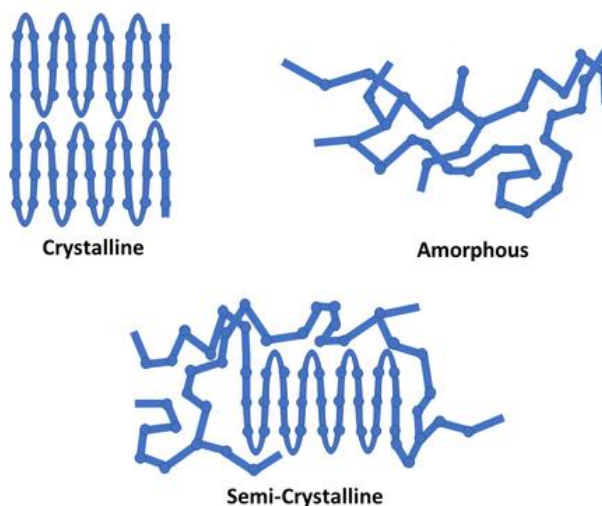


Figure 3 Polymer crystallinity types [3]

#### 2.1.1.4. Homopolymer or Copolymer

Depending on the composition, polymers can be homopolymers or copolymers. The former is characterized by being formed by a single type of monomer, while copolymers are formed by 2 or more types of monomers.

#### 2.1.2. Polymerization

The reaction by which polymers are synthesized is called the polymerization reaction. In a polymerization reaction, the various monomers are linked together forming the various chains that will eventually form the final polymers. There are two different types of polymerization reactions: addition and condensation polymerization.

In addition polymerization, the monomers join one after the other resulting in the polymer chain. While in a condensation polymerization, two monomers react to form a larger molecule with the simultaneous removal of a smaller molecule, like water. In this type of polymerization, the reactive species react through their functional groups [2].

## 2.2. Biodegradable Polymers

Although there is no clear definition of the concept of biodegradability, many authors agree that it is a degradation process from which a material breaks down through interaction with biological elements giving rise to natural products such as water, gases, salts, etc [4].

Therefore, biodegradable polymers are polymers that degrade due to its interaction with biological elements, such as enzymes, bacteria, fungi, etc. This process of degradation begins with the breakdown of the molecule into smaller parts through oxidation reactions, hydrolysis, etc. These smaller parts are then assimilated by the corresponding microorganisms or organs, which break them down into the various by-products. A very important aspect about the degradability of polymers is that it depends on several factors such as its chemical structure, the nature/origin of the polymer and the environment in which it is placed in [5].

In terms of structure, biopolymers are mostly made up of ester, ether and amide bonds. And it is this distribution of these links along the structure that will determine the properties of these polymers.

The properties of biopolymers are something that, in the same way as their basic structure, is shared by many of them. Among all the properties that these can present, the following could be highlighted:

- They are not toxic
- They are usually hydrophilic. In this way the enzymes can degrade its structure
- They are able to maintain their structure and mechanical properties until they begin to degrade
- Ability to control the degree and speed of degradation [6].

### 2.2.1. PVA

Poly(vinyl alcohol), better known as PVA, is a biocompatible and water-soluble synthetic polymer obtained from the hydrolysis of polyvinyl acetate. PVA is a polymer highly used in biomedical applications mainly due to its good biocompatibility, biodegradability, eco-friendliness and low toxicity [7].

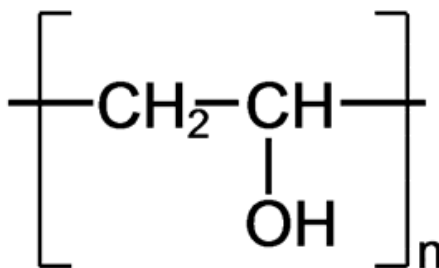


Figure 4 PVA chemical structure [8]

An interesting feature of PVA, although it is not exclusive to this polymer, is its ability to form hydrogels without the need for a crosslinking agent, through a freeze-thawing process. With this process, the solution freezes and thaws creating all the gel pores that will characterize the hydrogel.

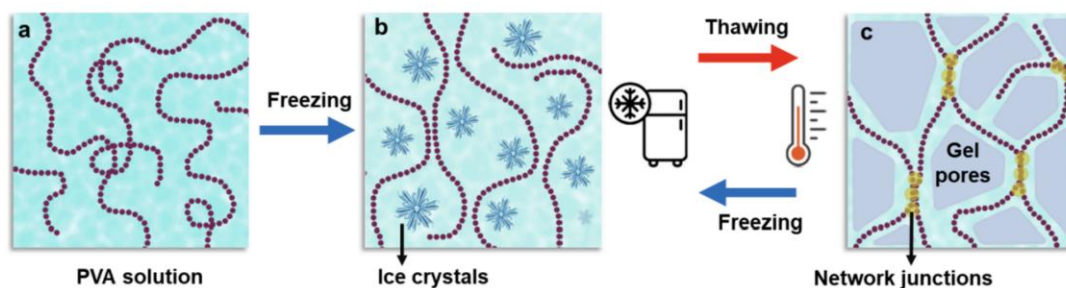


Figure 5 Freeze-Thawing method representation [7]

This characteristic, together with all the properties mentioned above, have been one of the reasons why it has finally been decided to use this material as the basis of the hydrogels used in this project. Even so, it has been necessary to add a series of additives to these hydrogels in order to provide them with the precise characteristics necessary to obtain a desired final product, for example, to improve the electrochemical properties of PVA hydrogels [7].

### 2.3. Conducting Polymers

For a long time, polymers were considered as insulating materials by nature but in the 70s, scientists Alan J. Heeger, Alan G. MacDiarmid and Hideki Shirakawa discovered several polymers that presented a high electrical conductivity when they were in the partially oxidized state. This discovery awarded them the Nobel Prize in Chemistry in 2000 for the discovery of "electronically conducting polymers" [9].

As the name itself indicates, conducting polymers are polymers that have the ability to conduct electricity in the same way that metals or inorganic semiconductors can [10]. Conducting polymers (CPs) are macromolecules that have a conjugated system of pi bonds, a structure that allows the delocalization of these electrons along the length of the molecule, providing it with the ability to conduct electricity [11].

Although this class of polymers has a high initial electrical conductivity, this can be increased through two processes: subjecting the polymer to oxidation process or modification of the polymer through addition of functional groups.

Aside from good conductivity, CPs present a wide range of other characteristics such as lightweight, good magnetic properties, good absorption of microwaves (widely used in aviation) and good optical and mechanical properties. Because of these, CPs are widely used in many sectors and industries in the world today [11].

Moreover, some CPs have also presented a very good biocompatibility properties that have caused them to be widely used in the biomedical sector, especially in the development of biosensors [10].

### 2.3.1. Polymer Doping

The conductivity of some polymers can be raised until reaching a similar point like metals by doing electrochemical doping, divided in n-doping (reduction) and p-doping (oxidation). It was discovered that the conductivity of a polymer could be increased by making it react with small quantities of electron-accepting or electron-donating species. That way, p-doping refers to the partial oxidation of a polymer and n-doping refers to the partial reduction of the CP [12].

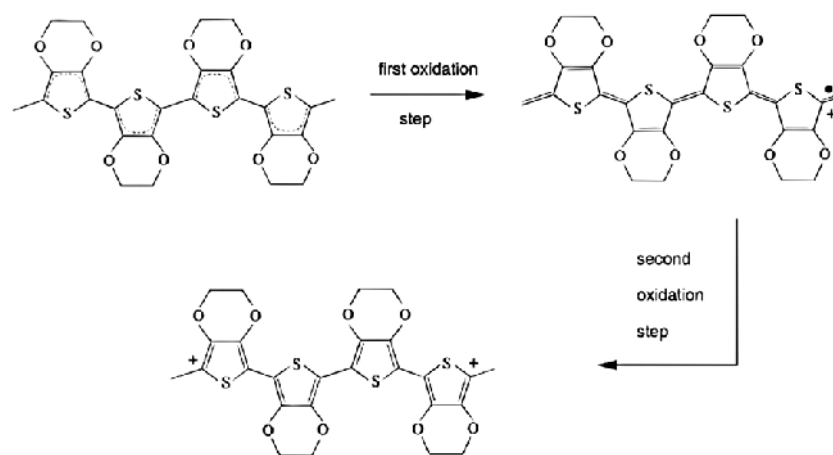


Figure 6 Representation of how doping work on CPs [13]

The type of dopant, the dopant strength and level, will determine the final conductivity of the CP.

### 2.3.2. PEDOT:PSS

Poly(3,4-ethylenedioxythiophene), also known as PEDOT, is a CP widely used in the biomedical field for its excellent biocompatibility. It is a transparent and very stable polymer that allows a high conductivity in its state but that has a couple of drawbacks to consider, one of them being its low solubility in aqueous environment [14]. Hence, to stabilize PEDOT in aqueous solutions, it is doped with poly(styrene sulfonate) or PSS.

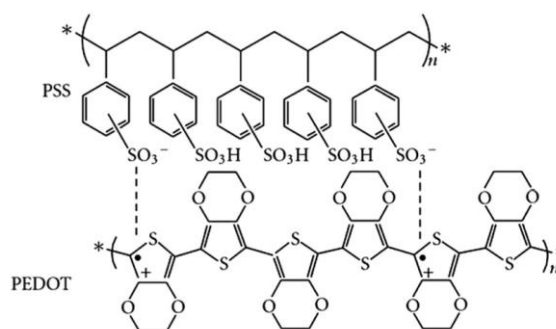


Figure 7 PEDOT:PSS chemical structure [15]

PEDOT:PSS (poly(3,4-ethylenedioxythiophene): polystyrene sulfonate) is a polymer composed of PEDOT (positively charged) and PSS (negatively charged). The addition of PEDOT:PSS to PVA hydrogels can produce several effects on the properties of the hydrogel such as improving its conductivity and enhancing the swelling properties of the hydrogel [16].

The other disadvantage of the PEDOT:PSS polymer is its low mechanical strength. This is a problem especially in those applications where good conductive properties are needed but the material/structure must be under mechanical stress (bending, compression, mobility, etc.), as in the case of this project with the fabrication of the conductive hydrogel for the electrode [16].

## 2.4. Hydrogels

Hydrogels are networks of hydrophilic polymers (crosslinked polymers) that are able to absorb and retain large amounts of water (in relation to their volume and weight) while maintaining their three-dimensional structure in a stable manner [17].



Hydrogels structure can be doped with some additives in order to improve their properties or give them some characteristics that initially did not have for example, improving mechanical strength, giving some hydrogels with the ability to conduct or improving their electrochemical properties, control the degradation, etc.

That way, tailored hydrogel structures can be obtained in order to be used in many biomedical applications.

## **2.5. Additives**

As said, in some cases, hydrogels will need to be doped with some additives in order to achieve the desired properties for a specific use. In this project, three studied additives will be used in order to be able to see their influence on the hydrogels and how these additives interact with each other (hydrogel structure, conducting properties or degradation).

The three additives studied in the project are the carbon quantum dots (CQD) and PEDOT:PSS which will be used to improve our hydrogel electrochemical properties (conductivity, capacitance, etc.) and tannic acid (TA) which will be used to obtain the desired mechanical properties as well as improve the electroactivity of the general hydrogel.

### **2.5.1. Carbon Quantum Dots**

Carbon Quantum Dots (CQD) are carbon nanoparticles with sizes that go below 10nm. Thanks to their size and structure, CQDs have a very good water affinity and can be dispersed in aqueous solutions. The term “quantum dots refers to a type of nanoparticle with the called quantum confinement which is an effect observed when the particle is too small to be compared to the wavelength of the electron [18]. Also these have become very popular in the because they are very abundant and inexpensive to fabricate, apart from a wide range of properties [19].

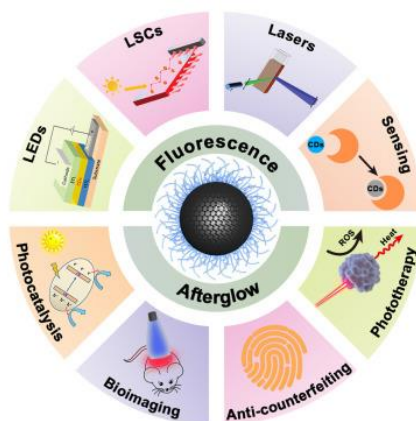


Figure 8 CQD applications scheme [20]

CQDs are considered to have superior biological properties as they have such low toxicity and great biocompatibility. In a study performed by Campuzano S., Yáñez-Sedeño P., Pingarrón, JM., CQD demonstrated also a good chemical stability, excellent dispersity and solubility, and efficient electrocatalytic performance [21].

CQDs have the ability to conduct electricity due to their highly conjugated carbon structures, which contain alternating single and double bonds. These bonds allow electrons to move freely through the CQD, allowing them to carry electrical current [22]. Their electroactivity is also being explored, as they have proven to be good electron acceptors and donors, endowing them with potential in optical and sensing applications [19].

For these reasons, they are now extensively studied in biomedical applications such as for bioimaging, biosensing, or drug delivery, to cite some examples.

### 2.5.2. Tannic Acid

Tannic acid (TA) is a polyphenol that can be obtained naturally from a wide variety of plants. Its chemical formula is usually given as  $C_{76}H_{52}O_{46}$ .

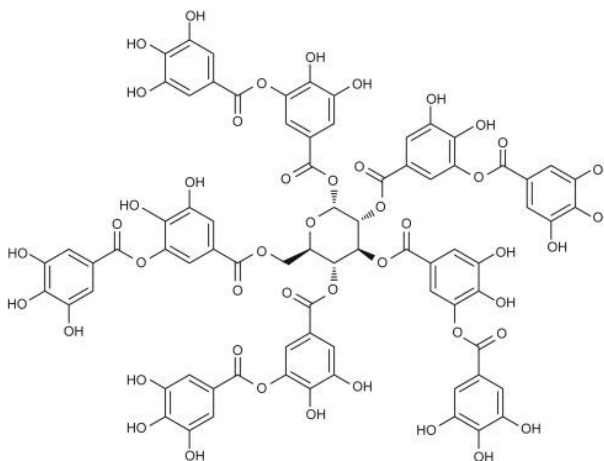


Figure 9 Tannic Acid chemical structure [23]

TA has a variety of valuable properties such as antibacterial, antioxidant, and the most relevant in hydrogel field, a good biodegradability. Another important characteristic of TA that makes it very special in hydrogel making is that it can provide multiple bonding sites, allowing the structure to form hydrogen bonds, ionic bonds and even hydrophobic interactions. These kinds of interactions provided by TA will enable hydrogels to have the desired structure and improve their mechanical properties [24].

## 2.6. TECHNIQUES

### 2.6.1. Cyclic Voltammetry (CV)

As the aim of this project is to build a hydrogel-based electrode to be used as a sensor (and characterize it), this hydrogel needs to have good electroactive properties. In this project, cyclic voltammetry was used to quantify the electroactivity of the hydrogel. Voltammetry is a type of electroanalytical method in which the information is obtained by measuring the current given by the sample as the potential is changed. Specifically, in this project, cyclic voltammetry has been carried out.

Cyclic Voltammetry (CV) is a commonly used electrochemical technique that provides us information about the oxidation-reduction processes of the studied species, the energy levels of the analyte and the kinetics of electronic-transfer reactions [25]. Hence, the electrochemical activity of the hydrogels could be characterized over time.

CV tests are composed of 3 fundamental electrodes: the working electrode (WE), the reference electrode (RE) and the counter electrode (CE). The working electrode, using a potentiostat, lineally

increases its potential until it reaches the maximum of the potential window, and then it reduces it until reaching the minimum. For this project, the potential window used was from -0.1 to 1 V. The reference electrode has a defined and stable potential equilibrium; hence it is used as a reference for the working electrode to apply the potential. Finally, the counter electrode is used to close the circuit by which the current created will circulate [25].

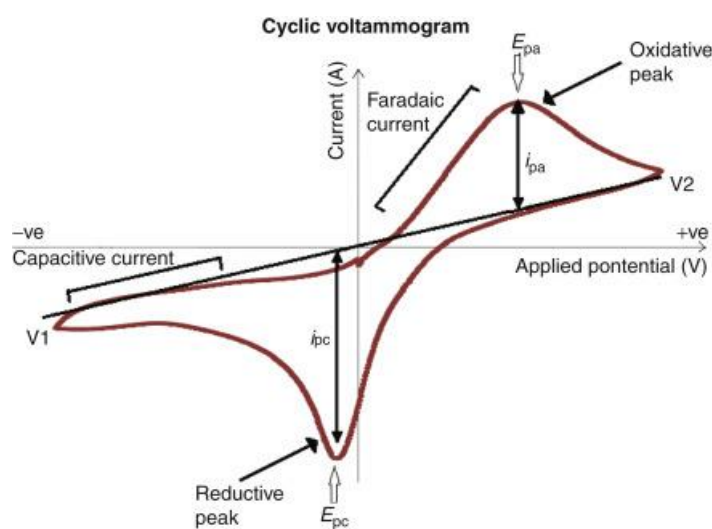


Figure 10 Example of a cyclic voltammogram [26]

At the beginning, an increasing reduction potential is applied and so the cathodic current increases (assuming there are reductive species in the solution/sample). Then, once all species in solution are reduced, the cathodic current decreases. That way information related to the redox potential and the speed of a reaction is obtained.

Cyclic voltammetry can be used to study a wide range of electrochemical phenomena, including electrocatalysis, corrosion, and electrodeposition. It is a powerful tool for characterizing the properties of electroactive materials and can be used in research and industrial settings [27].

### 2.6.2. SEM

The Scanning Electron Microscope (SEM) is a type of electron microscopy that uses a beam of electrons to scan the surface of a sample. This electron beam is usually emitted from a trigger containing a cathode with a filament, most often tungsten. The electron beam, accelerated in the vacuum chamber, is condensed using a set of several lenses and is concentrated to a diameter of between 0.4nm and 5nm [28].



Figure 11 PhenomXL Desktop SEM (left) and Neon40 Crossbeam (right) used to perform visual examination of the samples

When the beam of electrons interacts with the atoms of the sample, secondary electrons are produced. These secondary electrons are detected and then amplified to reconstruct an image [28].

SEM was used to visualize the superficial structures of the hydrogels, which could be correlated to the results obtained in the other tests.

### 2.6.3. RAMAN

Raman spectroscopy is a photonic technique that allows the characterization and identification of a material regardless of its state or nature. This technique is based on obtaining radiation scattered by a material when a beam of light is incident on it. This phenomenon, known as the Raman effect, is not affected by the molecular composition or structure of the sample [29].

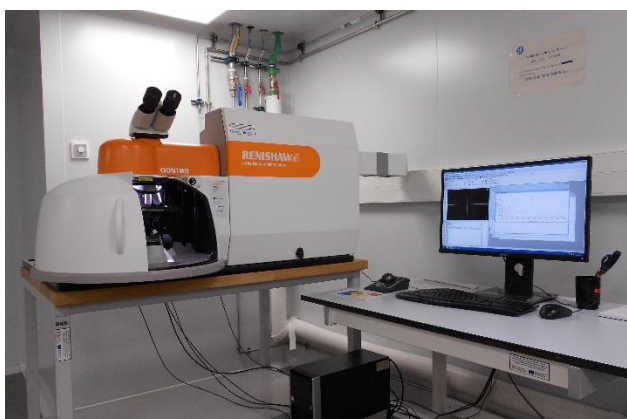


Figure 12. Renishaw's inVia Qontor Raman microscope

When a light beam of a certain frequency hits the sample, part of this light is absorbed and the other is scattered in multiple directions. The vast majority of this scattered light has a frequency equal to that of the incident light, but a small part of the light has frequencies different from the original. This effect is called Raman scattering and is characteristic of each molecule. The resulting spectrum show a series

of peaks that correspond to the different vibrational modes of the sample and can be used to identify the chemical bonds and molecular structure of the sample [29].

#### 2.6.4. FTIR

Fourier Transform Infrared spectroscopy (FTIR) is a technique that uses an infrared light to scan a sample in order to determine the presence of organic, inorganic and polymeric components in a sample. Each chemical bond in a molecule absorbs light at specific wavelengths, and the absorption patterns can be used to identify the presence of specific chemical bonds and functional groups in a sample [30].

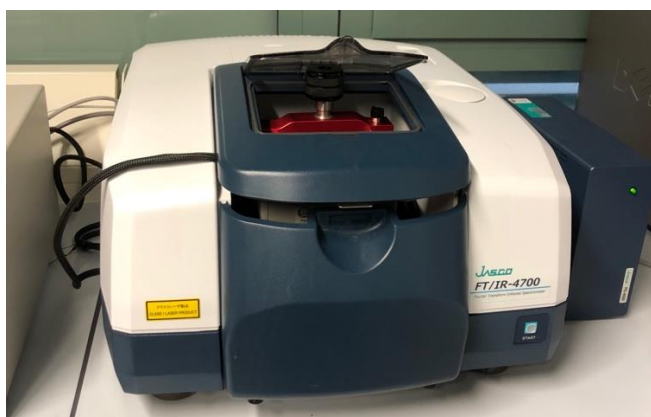


*Figure 13 Spectrophotometer FT/IR-4700 from Jasco Corporation*

As said, FTIR provides with information about the chemical composition of the sample. Some of the applications of FTIR spectroscopy include identifying unknown compounds, analyzing the chemical structure and/or quantifying the amounts of some compounds in a sample. The different functional groups present on the sample will be determined through the spectrum data and the used software [30].

## 3. EXPERIMENTAL METHOD

### 3.1. Methodology and Materials

For the methodology, all the procedures/protocols used in the project will be explained.

#### 3.1.1. Carbon Quantum Dots

The CQD were prepared using the hydrothermal method. 300mg of Chitosan (High Molecular Weight, >75% deacetylated) provided by Sigma-Aldrich were mixed with 30ml of 1% Acetic Acid solution from stock Acetic Acid Glacial solution ( $M_w = 60.052$ ,  $\geq 99\%$ ) from Fisher Chemical until dilution, and then was centrifuged at 12000 rpm for 10 min. The chitosan-acetic acid solution was poured into an autoclave and heated at 180 °C for at least 12h and then cooled to room temperature. The prepared solution was centrifuged at 4000 rpm for 15 min and then filtered using a 0.22  $\mu\text{m}$  filter. The as-prepared solution was heated at 90 °C until all solvent evaporated. The dried sample was then weighed and redispersed in Milli Q water depending on the desired CQD concentration.

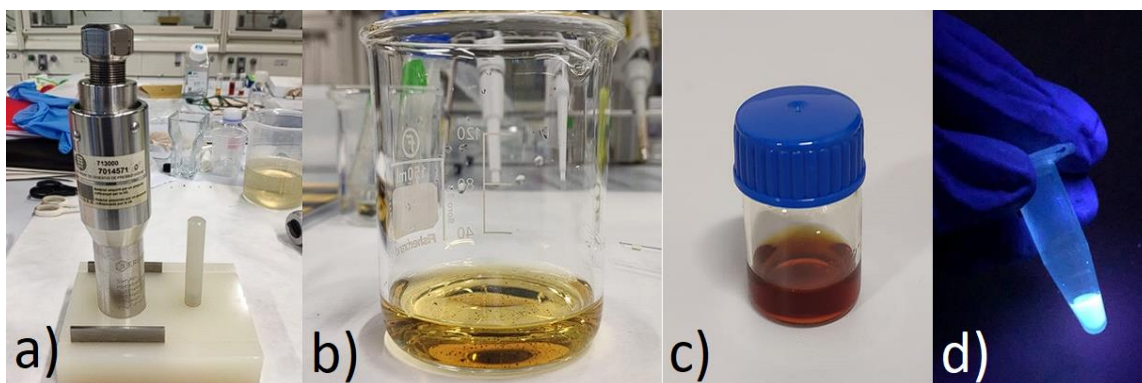


Figure 14. a) Autoclave used to heat CQD solution, b) CQD solution after 12h at 180 °C at the autoclave, c) CQD solution after solvent drying and redispersion in Milli Q water, d) CQD solution under UV light

#### 3.1.2. TA solution

The TA solution used in this project had a concentration of 20%. Hence, to prepare the desired concentration of TA solution a certain amount of Tannic Acid (ACS Reagent,  $M_w = 1,701.20$  g/mol) from Sigma-Aldrich was poured into milliQ water until obtaining a final 20% concentration solution.

### 3.1.3. Hydrogels

1g of PVA (MW: 61kDA, 98% degree of hydrolysis) was slowly added to a certain amount of Milli Q water to get a 10% PVA hydrogel, unless another percentage of PVA was needed. The mixture was stirred vigorously with a magnetic stirring bar and heated to 90 °C until all the PVA was dissolved and a homogeneous mixture was obtained. Certain amounts of 20% tannic acid solution, 1% CQD solution, and 0.65% PEDOT:PSS solution were then added separately to the PVA mixture and further stirred at room temperature for another 1 hour.

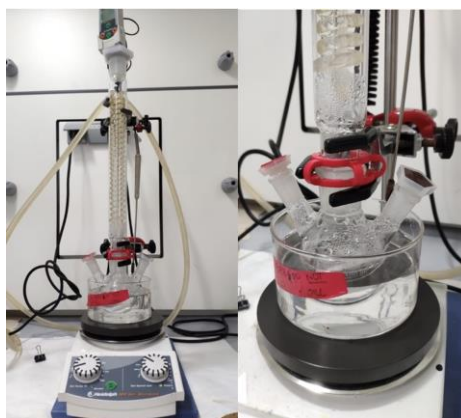


Figure 15 Assembly used for PVA solution preparation

The mixture was placed in molds (approximately 12g of final solution per plate), which were then placed in -20 °C for about 20 hours and then in 4°C for about 4 hours. This freeze-thaw cycle was repeated three times. After the freeze-thaw cycles, the hydrogels were washed in Milli Q water at least three times and kept in Milli Q water at 4 °C.

The percentages of each additive present in the hydrogels are shown in the next table (the percentage of the additives is referred to the final hydrogel weight):

Table 1 Percentages of each additive used in every hybrid and single component hydrogel

<b>HYDROGEL</b>	<b>PVA (%)</b>	<b>CQD (%)</b>	<b>TA (%)</b>	<b>PEDOT:PSS (%)</b>
<b>A (PEDOT:PSS + TA)</b>	10	0	0.4	0.65
<b>B (TA + CQD)</b>	10	0.04	0.4	0.65
<b>C (PEDOT:PSS + TA + CQD)</b>	10	0.04	0.4	0.65
<b>D (PVA only)</b>	10	0	0	0



**CQD only**

10 0.04 0 0

**TA only**

10 0 0.4 0

**PEDOT:PSS only**

10 0 0 0.65

**3.1.4. PBS**

PBS (Phosphate Buffered Saline) is a solution made out of salts that was used in this project to maintain the samples through the different tests and time points. PBS can be found commercially in different concentrations (1X or 10X normally) or can also be prepared manually. For this project, as large amounts of PBS were needed, it was prepared manually.

The next procedure was followed to prepare 1X PBS solution:

- Half of a 500ml volumetric flask was filled with Milli Q water.
- Using a spatula, the next salts were weighed and poured into the volumetric flask:
  - 4g NaCl
  - 100mg KCl
  - 720mg Na<sub>2</sub>HPO<sub>4</sub>
  - 120mg KH<sub>2</sub>PO<sub>4</sub>
- The volumetric flask was filled with Milli Q water and agitated until complete dilution of the salts. PBS solution is not recommended to be maintained on the fridge for more than 2 weeks.

## 4. HYDROGEL CHARACTERIZATION

In this section, the protocols and procedures followed for the hydrogel's characterization tests performed during the project are going to be explained.

The following table show the number of samples per hydrogel were tested during the project:

*Table 2 Total of samples testes per hydrogel and per test through the project*

<b>HIDROGEL</b>	<b>DEGRADATION</b>	<b>SWELLING RATIO</b>	<b>CV</b>	<b>FTIR</b>	<b>RAMAN</b>	<b>SEM</b>
<b>A (PEDOT:PSS + TA)</b>	33	33	30	2	2	4
<b>B (TA + CQD)</b>	33	33	30	2	2	4
<b>C (PEDOT:PSS + TA + CQD)</b>	33	33	30	2	2	4
<b>D (PVA only)</b>	33	33	30	2	2	4
<b>CQD only</b>	3	3	6	1	1	2
<b>TA only</b>	3	3	6	1	1	2
<b>PEDOT:PSS only</b>	3	3	6	1	1	2
<b>TOTAL SAMPLES TESTED</b>						<b>464</b>

For the degradation and swelling ratio tests it was decided to test 3 samples per hydrogel per time point, during the course of 8 weeks. As some more tests were done (7 days degradation test with 3 time points), that makes a total of 3 samples \* 8 weeks + 3 samples \* 3 days = 33 samples per hybrid hydrogel (and per test) in all the project. For the single component only 1 time point was studied and so only 3 samples per hydrogel were needed.

For the CV test a similar scheme was used, as 3 samples per hydrogel and time point were used. That makes a total of 3 samples \* 8 weeks = 24 samples per hybrid hydrogel in the project. As some other experiments were performed to correlate the data extra 6 samples per hydrogel were tested.

For the FTIR and Raman only two samples per hydrogels were tested, one sample of the Week 0 and another for the Week 4. Hence, a total of 2 samples per hydrogel and test were used. For the single component hydrogels, only a sample of the Week 0 were tested to correlate the hybrid hydrogels data.

Finally, for the SEM images a total of 2 samples per hydrogel and per week (Week 0 and Week 4) were tested. Hence, a total of 4 samples per hydrogel were tested in the project. For the single component, again, only 1 sample per hydrogel of Week 0 were tested.

## 4.1. CYCLIC VOLTAMMETRY

To perform the CV tests, as was already explained in the introduction, a potential was applied to the tested sample and the current given by it was measured using the different electrodes. To perform the tests a potentiostat-galvanostat (Metrohm, PGSTAT101) and the NOVA 2.1 software were used. For the CV test a total of 138 samples were tested during the project. Also, some liquid-state CV tests were performed (as can be seen on the section 5.1.2) to analyze additive effects on hydrogels.

### 4.1.1. Solid-State Cyclic Voltammetry

To perform the solid-state CV tests, hydrogels samples with an approximate surface of 3mm x 3mm were cut off.

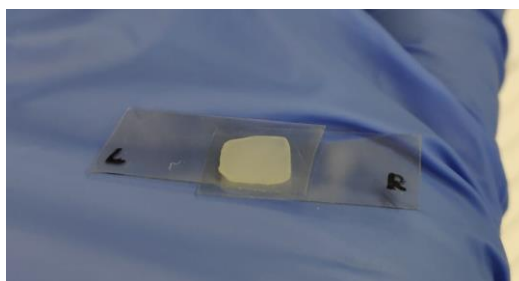


Figure 16 Hydrogel sample placed between ITO layers to perform CV

As shown in Figure 16, the sample was placed between two pieces of indium tin oxide (ITO)-coated PET, with the ITO sides in contact with the hydrogels. ITO coating results in the conductivity of the PET sheets. That way, the sample could be maintained between two conductive layers while connecting it to the assembly.

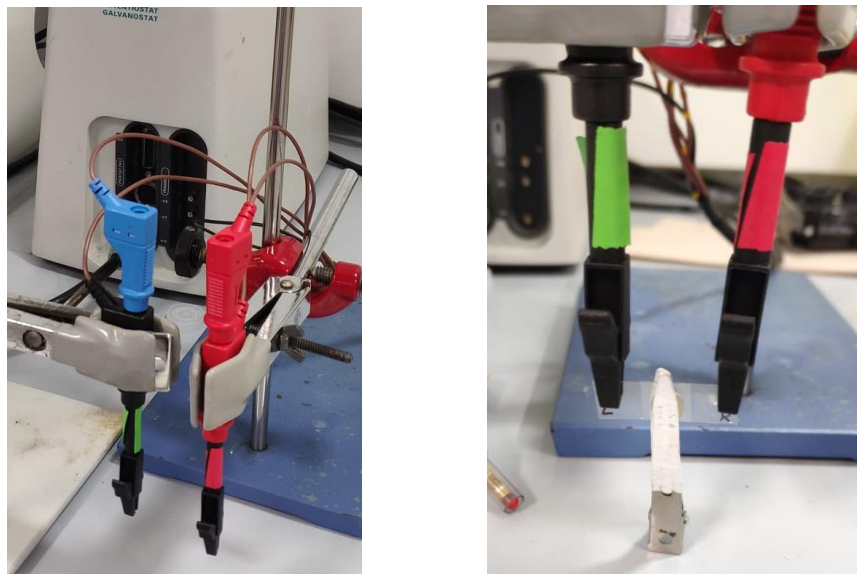


Figure 17 Assembly used for solid-state cyclic voltammetries

The solid-state CV assembly was made out of 2 stands, 2 crocodile clips to connect the sample and the electrodes (counter, reference and working). The same equipment was used through all the tests to minimize errors.

#### 4.1.2. Liquid-State Cyclic Voltammetry

When it was needed to test a solution, the following CV assembly was used:

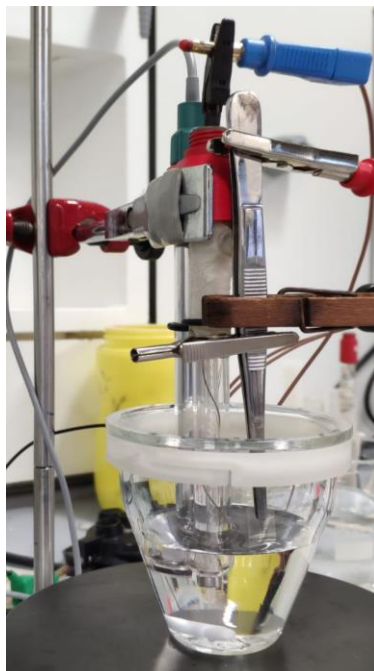


Figure 18 Assembly used to perform liquid-state cyclic voltammetries

The principle is the same as in the solid-state CV with the only difference that in this case a KCl solution was used as a supporting electrolyte in which to add the tested solution. In this case, an ITO layer was used as a working electrode to measure the given current. A platinum electrode was used as the counter electrode and an Ag|AgCl reference electrode.

The following parameters were used to perform the tests:

- **Start potential:**  $-0,1 V_{ref}$
- **Upper vertex potential:**  $1 V_{ref}$
- **Lower vertex potential:**  $-0,1 V_{ref}$
- **Stop potential:**  $0 V$
- **Number of scans:** 3 or 50
- **Scan rate:** 10mV/s, 50mV/s and 100mV/s

The specific capacitance (SC) was then calculated using the following equation:

$$\text{Specific Capacitance (SC)} = \frac{A}{2 \cdot m \cdot k \cdot \Delta V} \quad [28]$$

## 4.2. DEGRADATION

This project, as was explained at the beginning, was planned to characterize hydrogels meant to be used as electrodes for implantable sensors. Hence, it's critical to know how much the hydrogel is going to degrade inside the body through time. This is very important because as the hydrogel degrades, its conductive and mechanical properties are affected.



Figure 19. Sample preparation and storage for the swelling and degradation tests (left) and a hydrogel A (PEDOT:PSS + TA) dry sample after lyophilization

For the degradation test it was decided to cut 3 samples of each hydrogel per time point. Hence, a total of 141 samples were cut to obtain all data over the course of the project. All cut samples were then lyophilized. The initial lyophilized mass was then measured and taken as  $W_0$ . Samples were then placed inside Eppendorf tubes filled with 1.5 mL of PBS at pH 7.4 and placed in an agitator at 80 rpm and 37 °C. Before reaching each time point (approximately 1 or 2 days before), the samples were taken from the Eppendorf tubes and lyophilized for a second time. Once samples were lyophilized, they were weighed to obtain the degraded weight,  $W_{nd}$ . The degradation was then calculated per time point with the following equation:

$$Degradation (\%) = \frac{W_0 - W_{nd}}{W_0} * 100$$

### 4.3. CHARACTERIZATION TESTS

#### 4.3.1. Swelling Ratio

For the swelling ratio test, the same degradation test samples were used to perform the measurements. Hence, also a total of 141 samples were tested in this test.

To measure the swelled weight, at each time point, the degradation test samples were taken from the Eppendorf tubes and washed in milliQ three times to remove any salts or particles that could be on the sample. The excess superficial liquid was dried off and the swelled weight,  $W_{ns}$ , was measured. These samples were then lyophilized for the degradation test.

The swelling ratio was then calculated per time point  $n$ , using the following equation:

$$Swelling Ratio (\%) = \frac{W_{ns} - W_0}{W_{ns}} * 100$$

#### 4.3.2. SEM

In order to obtain some visual information about the structure and composition of the hydrogels, a morphological examination was done using the Neon40 Crossbeam™ FIB (Carl Zeiss) and the Phenom XL Desktop SEM (PhenomWorld). A total of 22 samples were tested (2 samples of each hybrid hydrogel per week (week 0 and week 4) + a sample of the single component hydrogels per week)

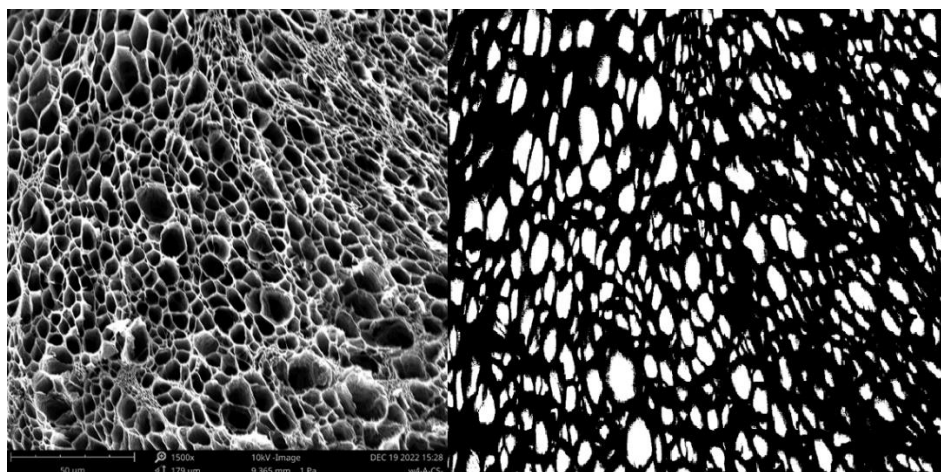


Figure 20 Hydrogel A (PEDOT:PSS + TA) SEM image (10kV, 1500x) and further ImageJ pore analysis

To obtain the various images, a range of voltages between 5kV and 20kV, and magnifications between 500 and 3000 were used. Once the images were taken, the ImageJ (National Institutes of Health, Bethesda, MD, USA) software was used to analyze pore size distribution and mean pore size of the different hydrogel samples.

To analyze pore size and distribution with Image J, a threshold was applied to the images to isolate the pores from the structure as can be seen on the right in Figure 20. After that, a mask was applied to the image and, using a particle size minimum threshold between 1 and 2  $\mu\text{m}$  (in order to avoid not pore shapes to be analyzed), pore measurements were obtained. To calculate the pore size distribution 3 images per hydrogel and per week were analyzed in order to have a wider range of data to perform the statistics.

The data extracted from Image J analysis was then processed and statistically analyzed using OriginLab software.

#### 4.3.3. FTIR

The characteristic peaks of each hydrogel were analyzed through the FTIR method. For this test the FT/IR-4700 spectrophotometer from Jasco Corporation (Japan) was used. For the FTIR, the same degradation samples were used to be studied. A total of 11 samples were tested. For the hybrid hydrogels 1 sample per week (week 0 and week 4) were tested and only 1 sample for each single component hydrogel was tested.

As the hydrogels studied in this project are made of PVA (present in all of them), TA, CQD and PEDOT:PSS the characteristic peaks of these materials should be expected to be found on the spectrums. For example, in the case of the PVA some peaks are expected to be found at around 3300

$\text{cm}^{-1}$ ,  $3000 \text{ cm}^{-1}$  and  $1100 \text{ cm}^{-1}$ , corresponding to the O-H stretching of the OH groups, the peak of  $\text{CH}_2$  and the C-O stretching of the ether respectively, as can be seen on Figure 21.

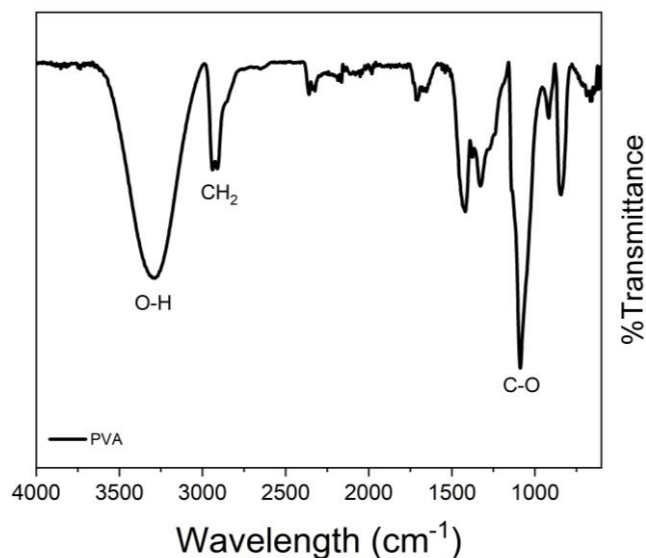


Figure 21 FTIR of the PVA only hydrogel on Week 0

For the FTIR tests the same degradation test samples (dried) were used. Small sample pieces were cut, introduced in the equipment and subjected to infrared wavelength energy. Data from spectra in the range of  $4000\text{-}600 \text{ cm}^{-1}$  was collected and corrected (noise and base-line) using an optimized software. The various peaks in the spectrum (corresponding to the various absorptions of the sample) represent the vibrational energies of the various functional groups present in the sample. For this test, a total of 11 samples were tested during the project.

#### 4.3.4. RAMAN

The purpose for this Raman test is to complement the FTIR data used to analyze the hydrogels structure. Hence, with both data the molecular structure and the chemical bonds of the samples can be identified and characterized. For the Raman spectrum, also a total of 11 samples were tested (following the same scheme as for the FTIR)

For the Raman test, the Renishaw's inVia Qontor Raman microscope and its Windows-based Raman Environment (Wire™) software were used to analyze the samples. A 785nm excitation laser was used, with an exposure of 10s and different powers in the range of 0.05 to 10 mW. That provided spectrums in the range of  $500 \text{ to } 4000 \text{ cm}^{-1}$ . Baseline and noise correction were done using the Raman software.



## 5. RESULTS AND DATA ANALYSIS

In this section, the results obtained in the different tests on the hydrogels will be discussed. Each characterization tests will be analyzed separately discussing the graphs figures presented correlating it with some other test data that can be relevant to explain some changes or deviations. At the conclusions, all data is going to be analyzed and correlated to find final answers to the stated objectives, and discuss possible sources of error as well as possible changes on methodology to obtain more/different data.

### 5.1. CYCLIC VOLTAMMETRY

#### 5.1.1. 3rd CV Cycle of Hydrogels (8-Week test)

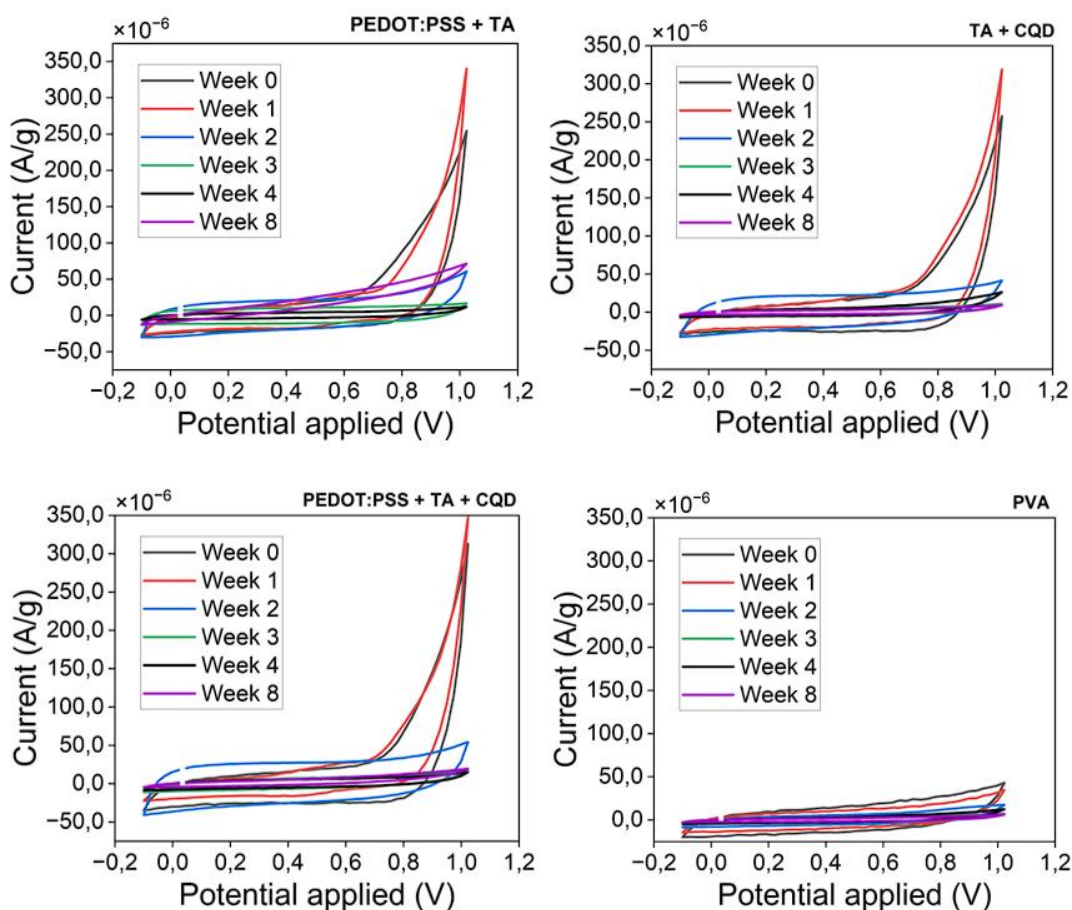


Figure 22 3rd Cycle CV of all hybrid hydrogels of the 8 weeks test

The graphs in Figure 22 have been obtained as a result of performing a 3-cycle CV with a scan rate of 50mV in each of the hydrogels, over 8 weeks.

The results shown here are the 3<sup>rd</sup> cycle for each 3-cycle test, as this is considered as the most stable peak cycle after the initial potential applications. This test was performed to determine the change in the electroactivity of the hydrogels over time.

The first observation that stands out most in these graphs is the two big oxidation peaks in the CV curves of weeks 0 and 1 of the hybrid hydrogels compared to the rest of the weeks. These CV curves are similar to the CV curves of the hydrogel containing only TA (Figure 36). In the same way, these oxidation peaks are not observable on the only PVA hydrogel CV as there is no TA on its structure (unlike the rest). That is why, a possible explanation for this effect could be that the peaks corresponding to these curves come from the TA present in the structure.

It can also be seen an increase between week 0 and week 1 on the current peak of all hybrid hydrogels. As samples have been stored for a week in PBS (and the week 0 samples for 24 hours), a hypothesis for this effect could be that the presence of salts in the hydrogel structure may increase the current peak on CV.

The results also show a decrease in the peak oxidation current reached after week 1. A hypothesis for this, is the rapid degradation of the hydrogels in the first weeks, as it can be seen on Figure 29. Through several visual inspections it can be observed how, in the first weeks, much of the hydrogel's TA was released into the medium in which the samples were kept (PBS), as the yellowness in the solution is observed. This could be another reason why the CV peaks got reduced from week 1.

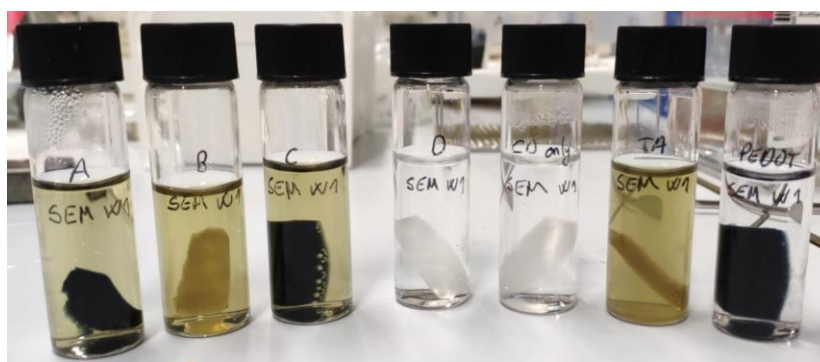


Figure 23 Visual test of TA release in samples of all hydrogel types preserved in PBS and agitation for 1 week. From left to right: Hydrogels A (PEDOT:PSS + TA + CQD), B (TA + CQD), C (PEDOT:PSS + TA + CQD), D (PVA only), CQD only, TA only and PEDOT:PSS only

CV data also shows a decrease in the area of the CV curves over the course of 8 weeks. This decrease in the area reflects the loss of electroactivity that samples suffered every week, related to the degradation processes that samples suffered over the time. As can be seen on Figure 29, samples suffer a degradation process from the first day after being stored in PBS, being the first days the ones that show the biggest degree of degradation (and stabilizing over the weeks). If the CV is analyzed again it can be seen how the curves decrease much more on the first weeks and the area decreasing stabilizes over time.

If a comparison between the graphs is made, the low conductivity of sample D (PVA only) can be highlighted, which is to be expected since it is the control sample. Taking this graph as a reference and the rest are compared, it can be seen that the addition of the additives has indeed produced a considerable increase in the electroactivity of the hydrogels.

In the same way, if the curves of hydrogels A (PEDOT: PSS + TA), B (TA + CD), and C (PEDOT: PSS + TA + CQD) are compared between them, it can be highlighted that hydrogel C is the one with the highest electroactivity since its curves have the largest area and highest curve peak, followed by hydrogel B. A similar behavior can also be seen on the SC data (shown on Figure 27) where the hydrogels B and C showed the highest SC values being the hydrogel A the one that obtained the lowest SC value (of the hybrid hydrogels).

### **5.1.2. TA and CQD solution CV**

Here, the results obtained by performing a CV on TA and CQD solutions of 1.5% concentration when adding volume of 50  $\mu$ l in 50 ml of KCl solution are discussed.

The idea with the TA and CQD solution tests is to be able to observe the influence of these two additives on the CV alone and mixed, and be able to correlate the information with the obtained on the CV 8-weeks test.

#### 1.5% TA solution CV

In Figure 24 the CV of 50  $\mu$ l of 1.5% TA solution in a KCl solution (used as a supporting electrolyte) is shown.

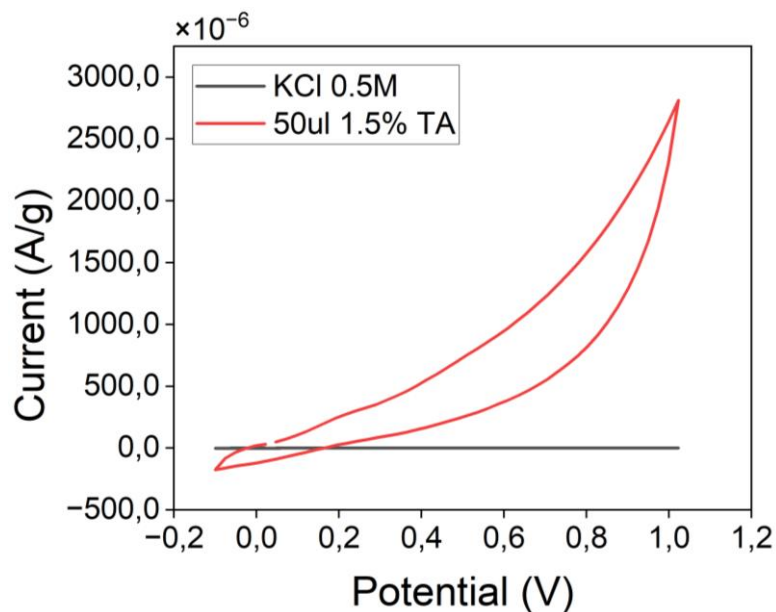


Figure 24 CV of 1.5% TA solution scanned at 50 mV/s using 0.5M KCl as supporting electrolyte.

The first observable effect is the clear increase in the peak current of the final solution, achieving a current of approximately  $2750 \times 10^{-6}$  A. If this value is compared with the values obtained in the hydrogel samples CV, it can be seen that the values in this test are almost 10 times higher. That effect is caused by the difficulties that additives have on the hydrogel structure to conduct electricity. In these tests (liquid-state CV) the additive present is moving through a solution, which makes the molecules easier to move and interact/react on the electrode's surface. That way, it can be seen how TA produced an improvement in the electrochemical properties of the solution, and so, we can confirm the improvement of the electroactivity of the hydrogels produced by the TA

Also, this TA solution peak shows some similarities with the peaks observed in the hybrid hydrogels CV in Figure 22. Hence, this data reaffirms the possibility of TA being the additive that produced those two peaks on weeks 0 and 1.

#### 1.5% CQD solution CV

In this figure, the CV of 50  $\mu$ l of a 1.5% CQD solution in a KCl solution can be observed.

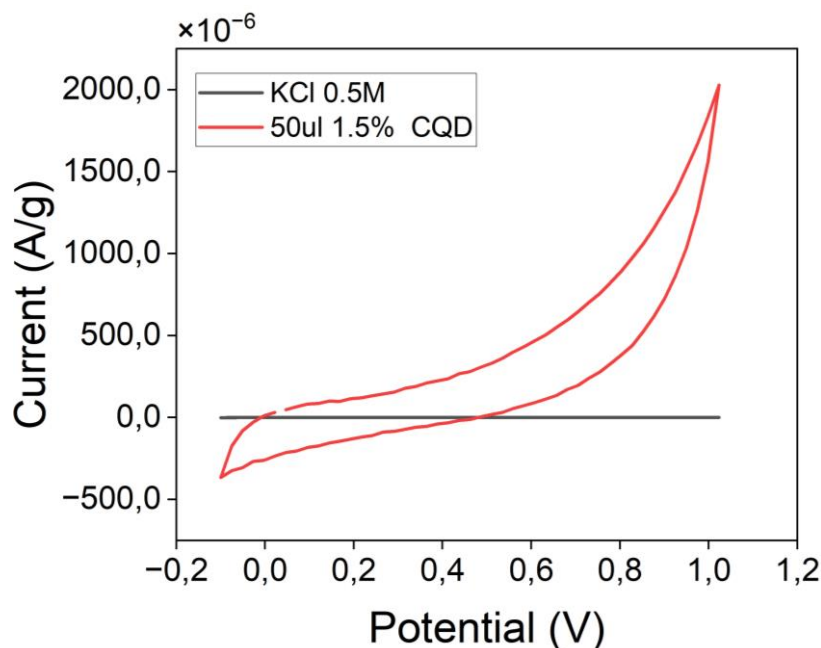


Figure 25 CV of 1.5% CQD solution scanned at 50 mV/s using 0.5M KCl as supporting electrolyte.

A similar response that the one shown in Figure 24 can be observed in this CV, as the addition of CQD increased the conductivity of the final solution obtaining an oxidation current peak of around  $2000 \times 10^{-6}$  A. Comparing the two maximum current peaks and the width of the CV curves areas it can be seen how the TA provided the solution with a better electrochemical improvement over the CQDs.

Hence, the TA showed to be a better electroactive component than CQDs, even though, both of them provided the solutions (and so the hydrogels) with an improvement in conducting and electroactive capacities.

Also, going back to the peaks of the CV in Figure 22 analysis, the possibility of the CQDs (or the CQDs interaction with TA) being the cause of that response can be refuted as the hydrogel A (PEDOT:PSS + TA) also presented those peaks and has no CQDs on its structure.

10% TA + 1% CQD solution CV

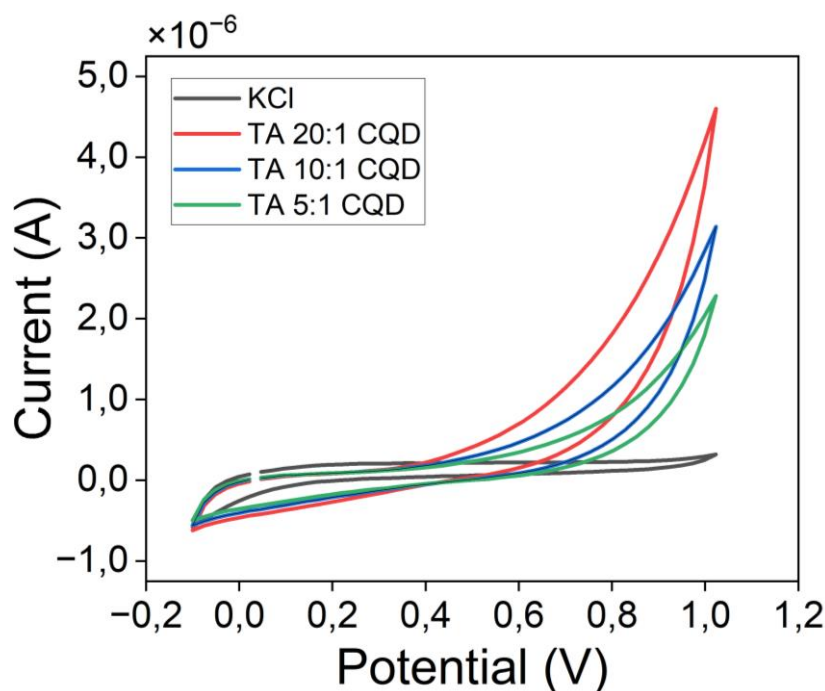


Figure 26 CV of TA and CQD at different ratios scanned at 50 mV/s using 0.5M KCl as supporting electrolyte

Finally, a CV test was performed on the combination of TA and CQD at different ratios to determine their synergistic behavior. Note that these CV curves are not normalized, hence a reduction in the current values is shown. The purpose of this test is to be able to see the response that the combination/interaction of the two additives show.

The first thing to note about the CV is the general behavior of the 3 curves. As can be seen, the maximum current peak is obtained with the highest TA to CQD ratio of 20:1 obtaining an approximate value of  $4.5 \times 10^{-6}$  A. On the other hand, the lowest peak current obtained was with the lowest TA to CQD ratio of 5:1. A hypothesis for this effect may be because by increasing the number of CQDs in the solution, they begin to interact with the TA present, causing a decrease in the electroactivity imparted by the CQDs and TA in the solution. As seen in the reviewed literature, the interaction between CQDs and TA can end up forming some spherical aggregates. Hence, the electroactive properties of both components may be a little disrupted by this interaction [32].

## 5.2. Specific Capacitance (SC)

### 5.2.1. 3rd Cycle Specific Capacitance (8 weeks test)

In Figure 27, the SC of all hybrid hydrogels during 8 weeks are shown.

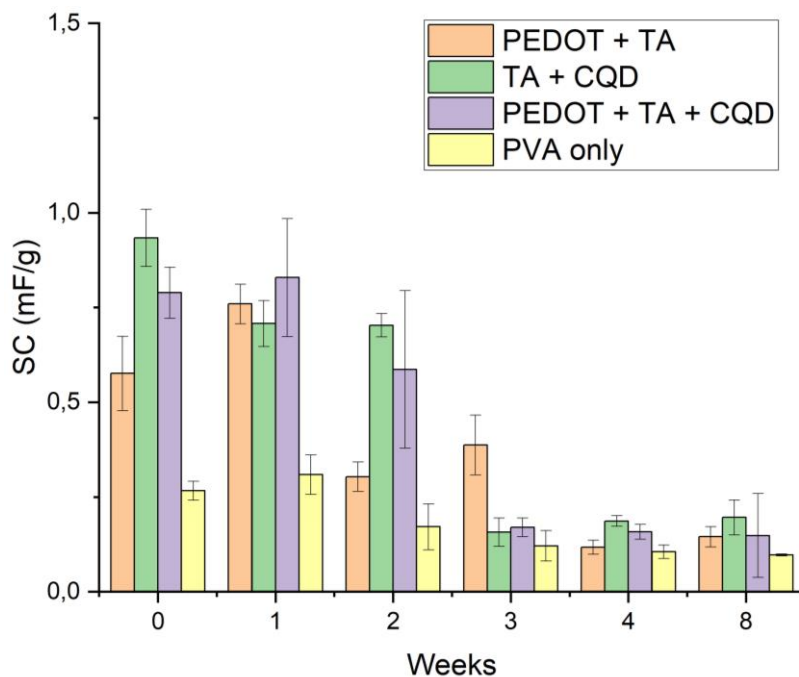


Figure 27 8 weeks SC (cycle 3) test of all hybrid hydrogels

The first observation that can be made is the general decreasing trend that all samples follow. This gives information about the degradation of the electroactivity of the samples during the weeks. The SC can be understood in a general way as “the capacity of the hydrogel to store energy”. Then, as samples degrade, that capacity decreases as structure is modified, and so the SC.

If the results are analyzed it can be seen how the maximum SC in almost all hydrogels were obtained on weeks 0 and 1, while the minimum can be found on weeks 4 and 8. Also, it is possible to see the stability of the SC from week 4 onwards. A hypothesis for that effect could be the stabilization of the degradation of the samples from week 4 to week 8, that can be observed in Figure 29.

Also, the effect of the additives added to the hydrogels can be observed on the first 2 weeks as there is a visible increase of the SC of all hybrid hydrogels compared to the PVA only one. From week 3, a big decrease of the SC is observed and all hydrogels (except for hydrogel A (PEDOT:PSS + TA)) obtained SC

values closer to the PVA only. This could give us more information about the degradation in the electroactivity of the additives that hydrogels suffered.

If SC data is analyzed through the weeks, a clear conclusion about the hydrogel with the highest SC cannot be obtained as maximum values of SC of the hydrogels change week to week.

A reason for those changes could be the effect that sample structure and degradation affects the SC of the sample. Changes in sample structure and composition (at the end, the physical properties) may produce some changes and effects on the SC of the hydrogels. Hence, some samples may have a higher SC on week 0 than others but, as it degrades faster, the SC decreases much more over the weeks.

Also, if hydrogel A (PEDOT:PSS + TA) and hydrogel C (PEDOT:PSS + TA + CQD ) are compared, it can be observed how the addition of CQD improved the SC, further showing the electroactivity imparted by the CQDs.

Finally, if the hydrogel A is analyzed alone, some fluctuations on the SC can be observed during the weeks. Since the results of the hydrogel A through the weeks (specially on the first 4 weeks) show an erratic behavior (increasing and decreasing from one week to the other), it is recommended to repeat this study to obtain better conclusions.

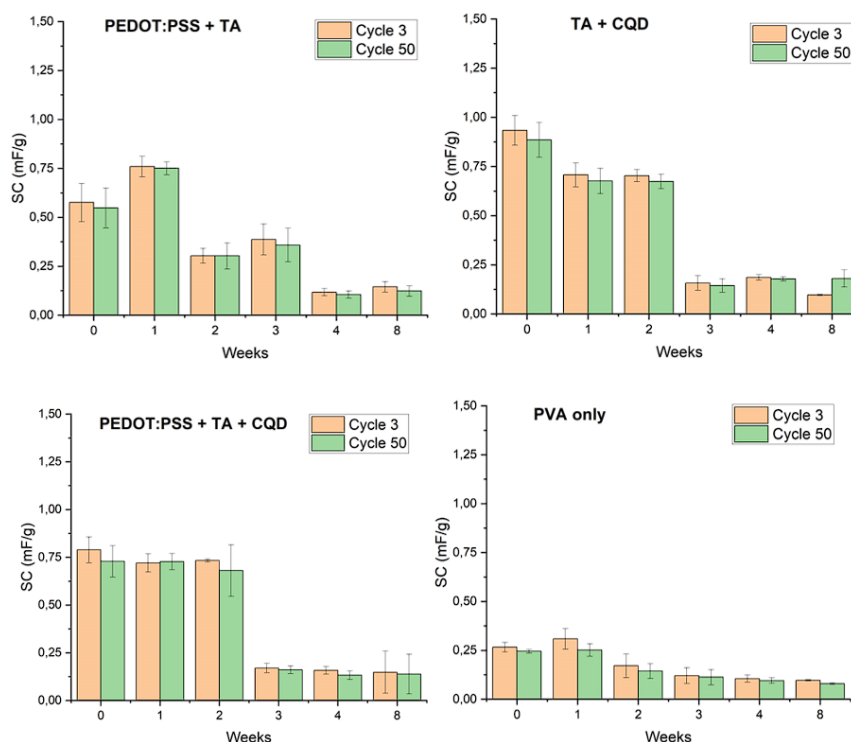


Figure 28 SC on cycle 3 vs cycle 50 of all hybrid hydrogels during 8 weeks



Finally, if the cycle 3 and cycle 50 SC values are compared, it can be seen how the number of cycles that samples underwent in the CV tests did not influence in the SC, as a small decrease from cycle 3 to cycle 50 is shown at every time point. Hence, it is recommended to repeat this study but making samples undergo more cycles in order to observe a biggest change in the SC.

### 5.3. Degradation and Swelling Ratio

#### 5.3.1. 8 Week Degradation Test

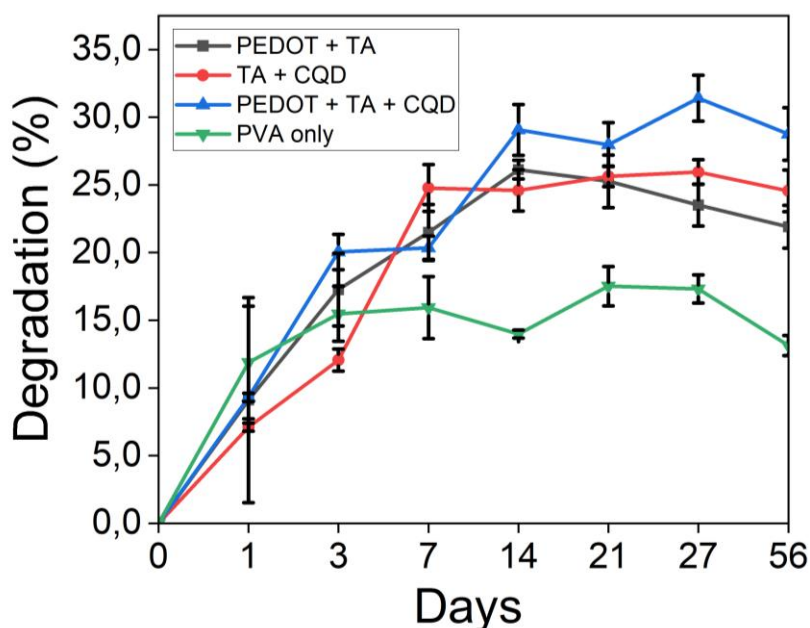


Figure 29 8 weeks degradation test of all hybrid hydrogels

The graph in Figure 29 was obtained after measuring the dry weight of samples that had undergone degradation for 1, 2, 3, 4 and 8 weeks.

The results show that the hydrogel C (PEDOT:PSS + TA + CQD) has the highest degradation throughout almost all the weeks with an approximate average of 29% degradation, followed by the hydrogel B (TA + CQD) and the hydrogel A (PEDOT:PSS + TA) with degradations of around 25%, and lastly the PVA only hydrogel with a degradation of approximately 16%. This last value is something that was expected since this is the sample that does not have any additives and therefore no conditions that could cause an accelerated degradation. On the other hand, it can be observed how by adding different additives to the hydrogel the degradation ratio increase.

A hypothesis for this effect is that the presence of the TA causes a higher degradation on the hydrogels. Because of its structure, when hydrogels are being prepared and gelled, TA could form hydrogen bonds with PVA, CQD and PEDOT:PSS, forming the hydrogel structure. As it could be seen on Figure 23 there's a clear TA release from the hydrogel structure to the medium. As a consequence, the released TA may have detached additives with which it was linked as well as part of the PVA that forms the hydrogel, leaving part of the internal and external structure exposed, thus causing further degradation. That may be the reason why all hydrogels except for the one that has only PVA had higher degradation, being the hydrogel C (PEDOT:PSS + TA + CQD) the one with the highest value.

Another possible hypothesis that can explain the trend in degradation can be found by looking at Table 4, showing that hydrogel C also has the highest pore size. That way, a correlation between pore size and degradation can be seen as bigger pore shows, on first instances, a higher degradation degree.

Comparing the hydrogels B and C another observation that can be taken. As the hydrogel that showed the highest degradation and had the biggest pores presented PEDOT:PSS on its structure, may indicate that PEDOT:PSS may be an important influencer on hydrogel degradation. Also, comparing the hydrogels A, B and C, it can be seen on the figure how CQD produced a clear effect on both degradation and pore size where hydrogels with CQD present on their structure degraded more than those that don't have it.

The next thing to discuss are the deviations present in the measurements of day 1. This could be because the samples of the same hydrogel in the first moments are degrading at different speeds.

Although attempts were made to simulate to the same fabrication and conditions between each sample, there will always be some differences between the samples that could lead to deviations in the first days of degradation. This could be the reason why the degradation values of days 3 and 7 of the samples of the same hydrogel ended up obtaining the same degradation values, and therefore the deviations in the measurements are highly reduced.

Something that is necessary to analyze is the PEDOT:PSS + TA hydrogel. If it is analyzed alone again (Figure 29) it can be observed how the degradation value decreases (specially from day 14). This is something that should not be expected as it indicates that the samples are gaining weight. The sources of this deviations may come from the experimental procedures. As it was explained in the methodology sections, the values for this test were obtained manually by weighing the samples. Hence, some initial weight errors were produced (bad calibration for example) and therefore, the final degradation values

deviated from what should be expected. Just to point out, changes of a couple of micrograms can lead to a change in the percentage of degradation of 5-10%, when dealing with samples of such a small weight.

In this case, it would be necessary to repeat the degradation test for the samples of this hydrogel.

### 5.3.2. 8 Week Swelling Test

After 8 weeks the following results were obtained for the swelling ratio of the hydrogels:

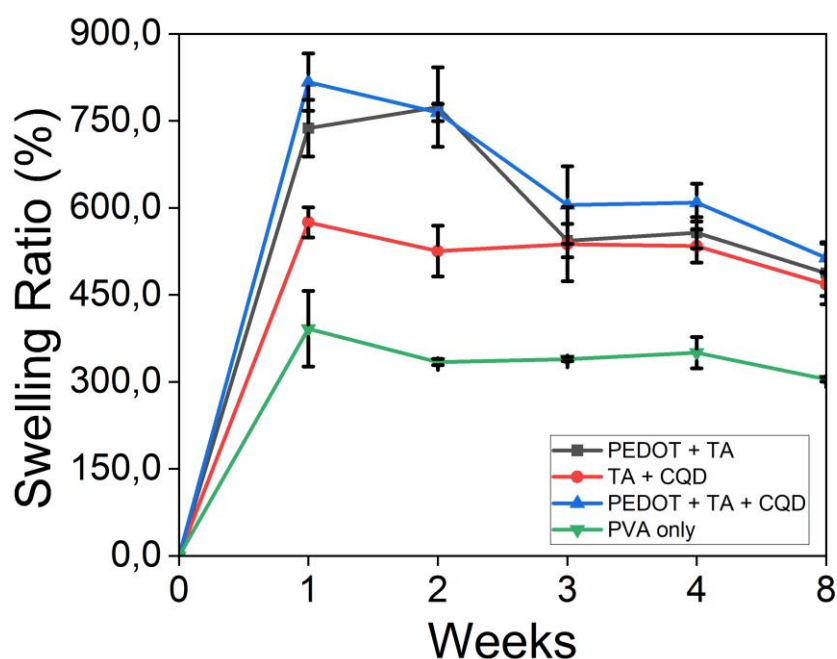


Figure 30 8 weeks swelling ratio test of all hybrid hydrogels

If Figure 30 is analyzed in general, several conclusions can be drawn. The first thing that stands out the most is the passage from week 0 to week 1 without a progressive process of the values. This is because the samples during the first week have absorbed all the volume of liquid they can contain.

It can also be observed that the swelling values decrease over the weeks. This effect may be related to the degradation process that the samples undergo when exposed to the PBS medium. If Figure 29 and Figure 30 are compared, a relation between them can be observed. When the degradation of the samples increases, the swelling gets reduced. Also, it can be seen how from week 1 the values from both swelling test and degradation slightly stabilize.

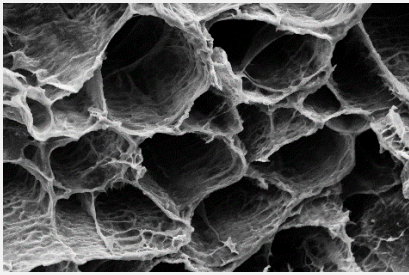
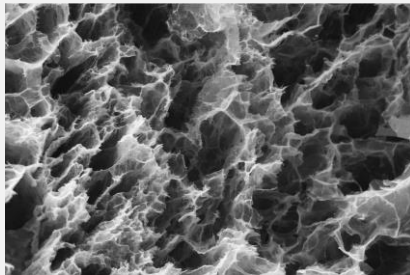
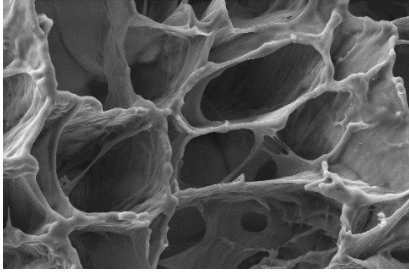
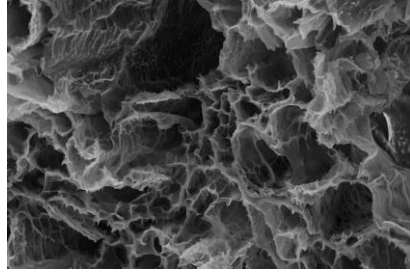
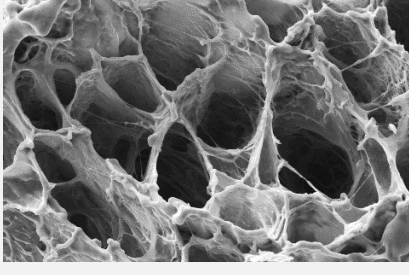
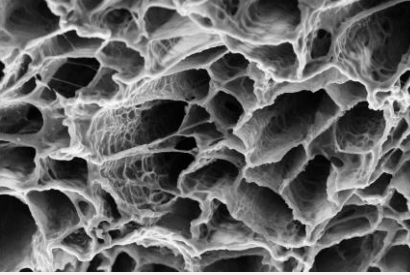
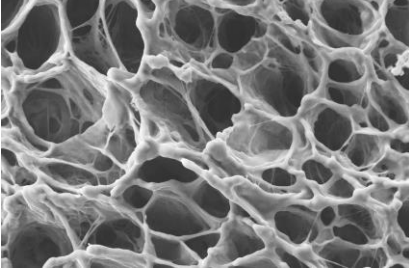
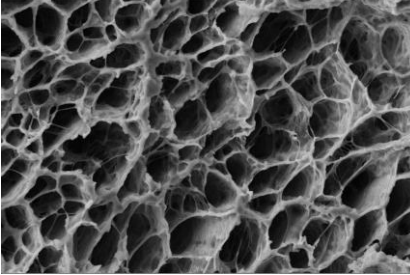
If the swelling values of each of the hydrogels are analyzed, it can be seen that hydrogel C (PEDOT:PSS + TA + CQD) is the one with the highest swelling, while the hydrogel with PVA only has the lowest value. This, in the same way that has been observed in the CVs and the degradation test, is something to be expected since the hydrogel with PVA only does not present any additive that could have altered its structure. It should also be noted that the hydrogels that have obtained greater swelling have been those that present PEDOT:PSS in their structure, which may indicate that PEDOT:PSS may increase the inner empty volume of the sample. Another hypothesis related to the swelling ratio values could be the relation with the pore size distribution of the different hydrogels. In the 5.4 section this relation will be discussed.

These results, although they have provided us with very relevant information on the swelling of the various hydrogels, were considered a bit unsatisfactory as high fluctuations in some hydrogel data can be found at some timepoints. These fluctuations may come from different sources such as the methodology used to weight the samples (when drying the superficial water prior to weighing) or the low efficiency of the lyophilizer on the time the samples were dried. As the conditions of the equipment were not stable during all the experiment some samples may have experienced some kind of structure damage (influencing then the physiological properties of these). Also mention, as done in the degradation section, that as dry samples weight is so low small differences in the measured weight may induce in big changes on swelling percentages.

## 5.4. SEM

In the following table the four hydrogel types are visually compared through SEM images on Week 0 and Week 4 to see any visible changes on structure. All images have the same 3000 X magnification in order to be able to compare the pore size and structure more precisely.

Table 3 SEM images of all hybrid hydrogels on week 0 and week 4 taken with a 3000x magnification and intensities between 5 and 15 kV

	WEEK 0	WEEK 4
<b>PEDOT:PSS + TA</b>		
<b>TA + CQD</b>		
<b>PEDOT:PSS + TA + CQD</b>		
<b>PVA ONLY</b>		

#### 5.4.1. Pore Size and Distribution

The Table 4 shows the mean pore diameter of all hybrid hydrogels on week 0 and after 4 weeks had elapsed.

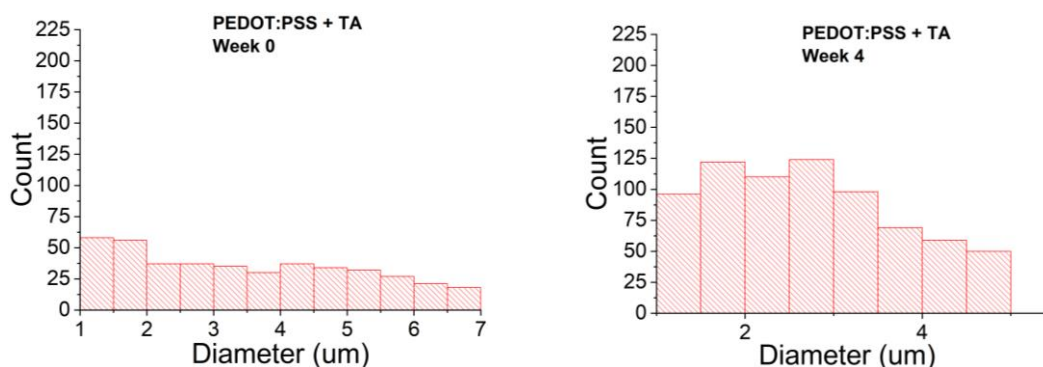
	WEEK 0	WEEK 4
<b>PEDOT:PSS + TA</b>	3,49 ± 1,68 μm	2,73 ± 1,03 μm
<b>TA + CQD</b>	2,32 ± 0,95 μm	2,07 ± 0,68 μm
<b>PEDOT:PSS + TA + CQD</b>	2,75 ± 1,15 μm	2,21 ± 0,80 μm
<b>PVA ONLY</b>	2,09 ± 0,69 μm	1,73 ± 0,41 μm

Table 4 Hybrid hydrogels mean pore diameter on weeks 0 and 4 with standard deviations

In this table some basic conclusions can be taken related just to the pore sizes. The first observation that can be made is that hydrogel A (PEDOT:PSS + TA) presents the biggest pore size with a mean value of 3,49 μm, followed by the hydrogel C (PEDOT:PSS + TA + CQD) with 2,75 μm, then the hydrogel B (TA + CQD) with 2,32 μm and finally the PVA only hydrogel with a pore diameter of 2,09 μm.

Also, in Table 4 it is possible to see the decrease that hybrid hydrogels samples have undergone after 4 weeks, as the pore sizes have decreased in all of them but maintaining the same order in terms of pore diameter sizes.

However, to be able to extract more precise conclusions it is necessary to also analyze the pore diameter distribution. In Figure 31 the pore diameter size distribution of all hydrogels on weeks 0 and 4 is shown:



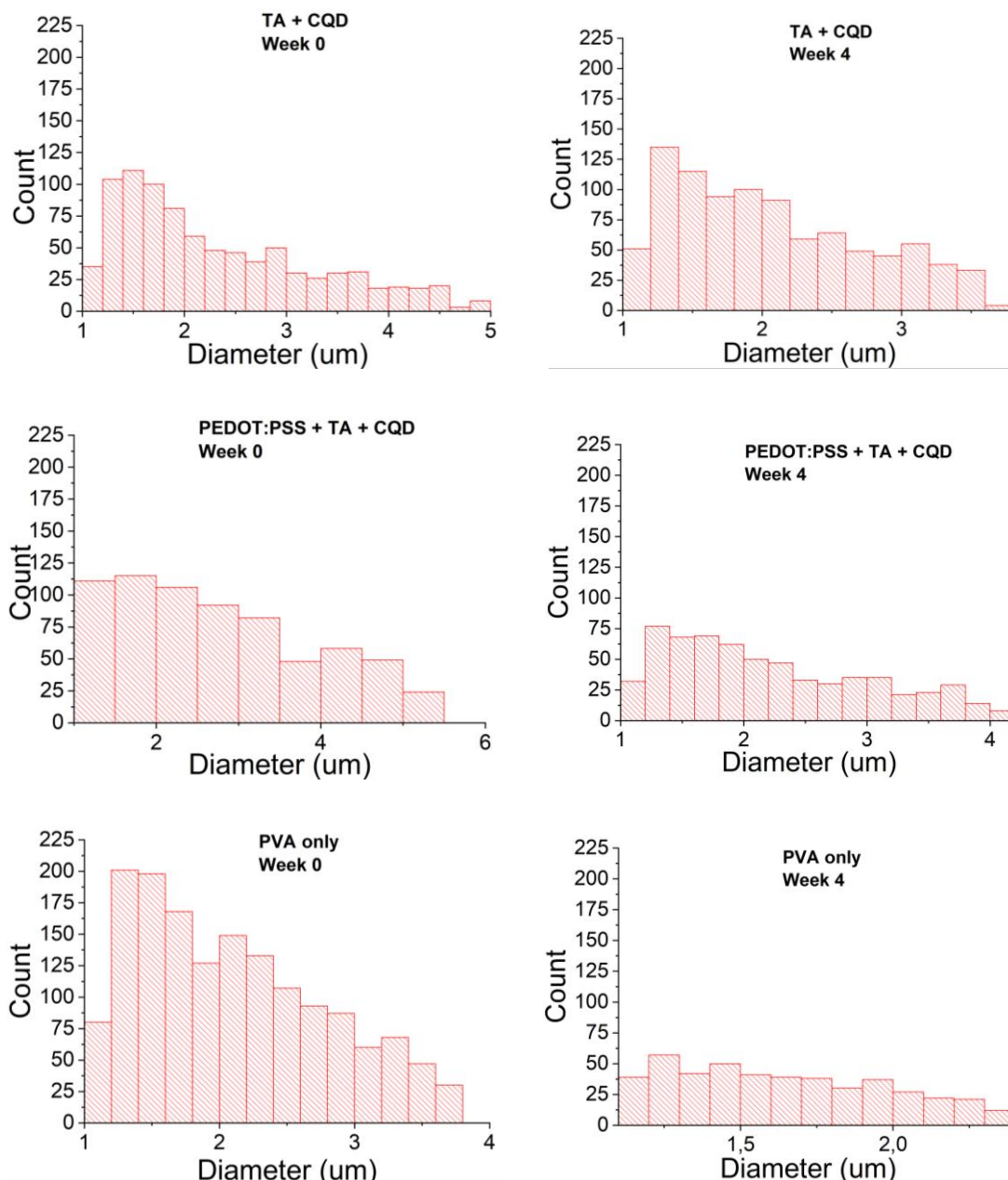


Figure 31 Pore diameter size histograms of all hybrid hydrogels on week 0 (left) and week 4 (right)

As it can be observed, all histograms follow the same behavior. The number of small pores is much higher than the big pores.

At this point, with all pore size data visible, the correlation between tests and samples can be seen. The first thing to note is the effect that PEDOT:PSS produces on the hydrogel structure. As it can be seen on Table 3 SEM images of all hybrid hydrogels on week 0 and week 4 taken with a 3000x magnification and intensities between 5 and 15 kV the hydrogels that have this additive presented a much rounded

pore structure, unlike the rest of the hydrogels that show a much compact one. That could be a reason why the hydrogels with PEDOT:PSS present on their structure have bigger but less pores.

In the other hand, the hydrogels B (TA + CQD) and PVA only presented the smaller pore diameters but the larger amount of them. A reason for that effect could be the structure of the hydrogel linking much more with itself and so creating more pores but smaller.

If this data is now compared next to the swelling ratio some hypothesis can be taken. A relation between pore size and swelling can be highlighted, as the hydrogels that obtained the higher swelling ratios are those that present the biggest pores on their structure (being also the ones that have PEDOT:PSS on their structure). Hence, it is shown how this additive produced some structural changes on hydrogels (producing then an effect on their physiological properties).

Another observable effect is the swelling of the hydrogel C (PEDOT:PSS + TA + CQD) that, even though it has the second larger pore diameter, the number of pores is much higher than for example on the hydrogel A making the total pore volume bigger. That could be a reason why those samples swelled the highest amount. On the other hand, we see a similar effect on the hydrogel B where, even though it has larger pores than hydrogel A, the total amount of pores may produce a higher inner volume on the hydrogel to be swelled.

Another effect to comment is the swelling of the samples with TA. During the preparation of the hydrogels with TA + CQD, TA seemed to make the structure much compact which should produce an effect on the swelling ratio decreasing it. But what can be seen it is the opposite. An explanation to that effect could be the linking between TA and the other additives that, instead of reducing the pore size it actually increases it. Related to this effect, that may be the reason why the hydrogel with all the additives reached the highest swelling ratio of all hydrogels, being the PVA only hydrogel the one that obtained the lowest. Also, as TA can interact with the other additives, these interactions may end up producing a much porous structure in the hydrogel.

If Table 3 Week 4 column is observed, it can be seen how the samples suffered a clear degradation during these 4 weeks. As it can be seen, especially on hydrogels A and B, the structure of the pores seems to be less rounded and "hairier" than on week 0. Also, analyzing the Figure 31, a clear reduction on the pore size is shown, as in some images the number of pores seems to have increase but their size has been reduced. Then, through this visual inspection and all the characterization tests data, it can be reaffirmed that samples have undergone a clear degradation through the 8 weeks. Also, if all



hybrid hydrogels images are analyzed it can be seen how the hydrogel's C pores maintained much better their rounded shape than hydrogels A and B. This effect, as it is only observed in this hydrogel, could be given by an interaction between PEDOT:PSS and CQD, which may induce in some hydrogel structure changes. That could be related with the higher values on the swelling ratio test.

## 5.5. FTIR

In Figure 32 FTIR spectrums of the different hydrogels on Week 0 (initial state samples) and Week 4 are shown.

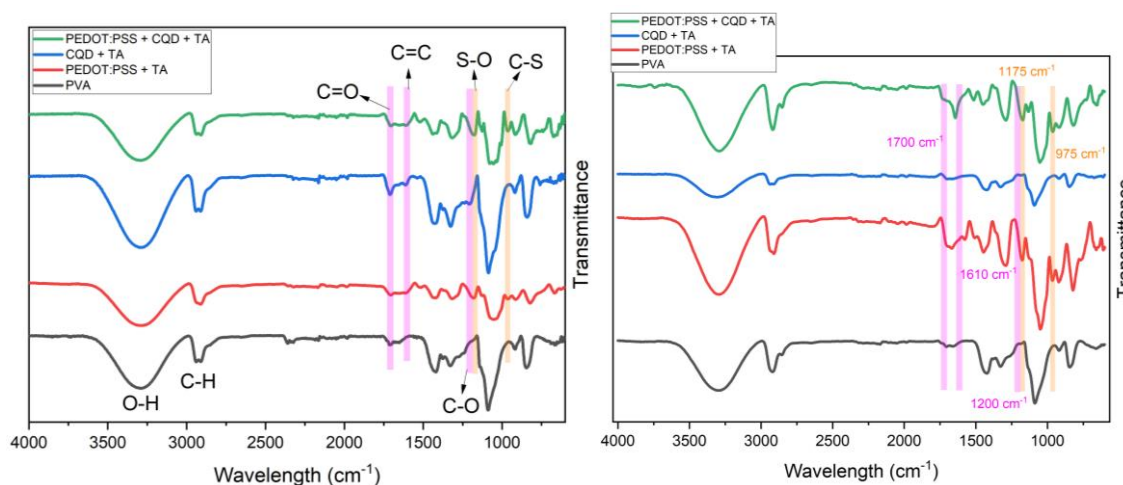


Figure 32. Week 0 (left) and Week 4 (right) FTIR of all hybrid hydrogels

In week 0 FTIR (left), the characteristic peaks of the PVA can be found at around  $3300\text{ cm}^{-1}$ ,  $2900\text{ cm}^{-1}$  and  $1100\text{ cm}^{-1}$  corresponding to the O-H, C-H and C-O stretching respectively. As all the hydrogels are made of PVA, these peaks can be observed in all FTIR spectrums [33].

If the different spectrums are analyzed, some characteristic peaks corresponding to the additives can be found. Although the spectrums in all hydrogels look very similar to the PVA only, some new peaks are displayed at around  $1700\text{ cm}^{-1}$ ,  $1610\text{ cm}^{-1}$  and  $1200\text{ cm}^{-1}$ . The band located at  $1700\text{ cm}^{-1}$  is characteristic of the C=O stretching of the acid/acyl esters, the peak located at  $1610\text{ cm}^{-1}$  is characteristic of the C=C stretching and the  $1200\text{ cm}^{-1}$  band corresponds to the C-O stretching in O=C - C groups. If now the Figure 9 is observed it can be seen that these 2 last peaks are the ones that indicated the presence of TA in the structure [34][35].

If PEDOT:PSS + TA + CQD and PEDOT:PSS + TA hydrogels spectrums are analyzed, two peaks can be found only on these two hydrogels spectrums (Figure 32) at around  $1200\text{ cm}^{-1}$  and  $975\text{ cm}^{-1}$  corresponding to the S-O and C-S vibrations of the thiophene ring [36].

For the CQDs, no characteristic peaks were observed on the FTIR obtained. A hypothesis for this effect could be the low concentration of CQDs on the hydrogels. Also, as CQDs characteristic band are located at the same peaks as other additives, the presence of CQDs cannot be confirmed just by the FTIR. [38] Hence, a visual inspection was done using a UV light lamp to determine the presence of CQD, thanks to their fluorescence properties. As it can be seen on Figure 33 the hydrogel reacted to UV light which indicates de presence of CQD on it.

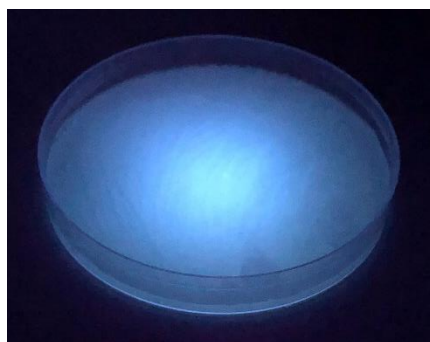


*Figure 33 CQD + TA hydrogel fluorescence under UV light to test visually the presence of CQD.*

Finally, if we compare the data from week 0 and week 4 some peak reductions can be observed in all hydrogel's characteristic peaks, especially on the TA + CQD hydrogel. A hypothesis for those peak reductions could be the degradation of the sample. Every PBS change that was made on the samples was carrying out part of the structure of the hydrogels and also the additives that were not attached.

Also, on hydrogels with PEDOT:PSS + TA and PEDOT:PSS + TA + CQD its possible to observe an increase on transmittance. This effect is something that should not be expected as samples have undergone a degradation process and so the transmittance was expected to be lower at week 4 samples. Those variations may be a result of various factors such as the sample purity, sample thickness (the thicker the sample the higher the transmittance) and also the methodology used to perform the IR. As the samples were placed manually in the equipment, maybe some samples were more pressed than other changing that way the transmittance given. Also, some software correction processes (baseline and noise correction) that are done by hand may have influenced on final results.

## 5.6. RAMAN

In this section, the Raman data is going to be analyzed. As it was explained in the introduction the Raman technique is going to be used to complement de FTIR data for the structure and chemical characterization of the samples.

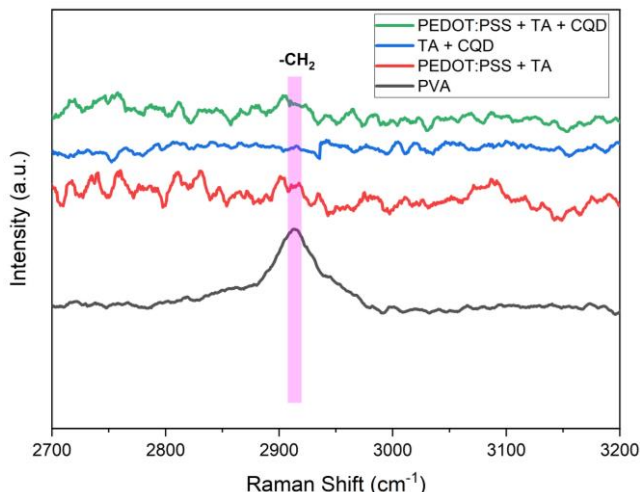


Figure 34 Week 0 Raman spectrum of all hybrid hydrogel from 2700  $\text{cm}^{-1}$  to 3200  $\text{cm}^{-1}$  to observe the PVA peak

As it can be seen on Figure 34 and Figure 35 two peaks at around 1400  $\text{cm}^{-1}$  and 2900  $\text{cm}^{-1}$  can be observed on the PVA hydrogel corresponding to the stretching vibration of  $-\text{CH}$  and  $-\text{CH}_2$  respectively [39].

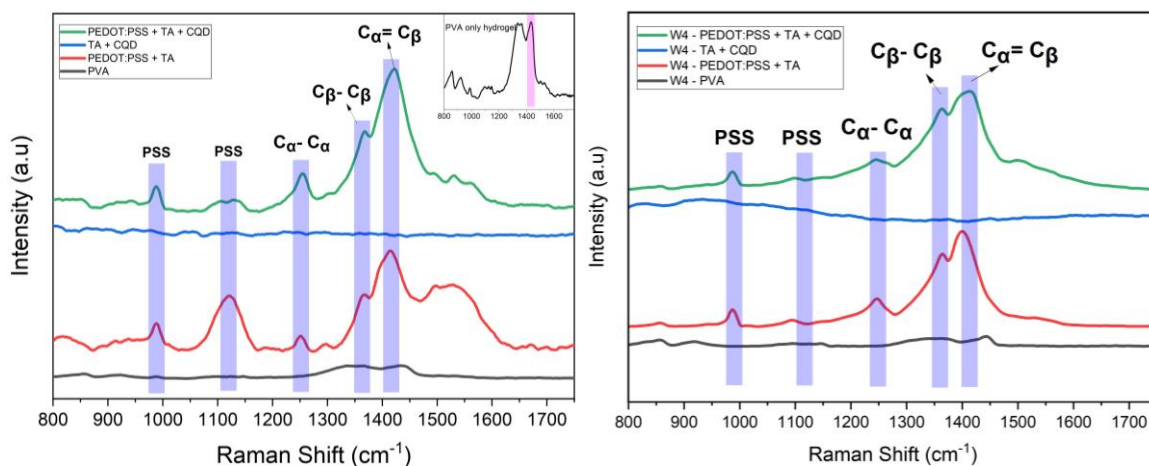


Figure 35 Raman spectrum from 800 to 1750  $\text{cm}^{-1}$  to show the PEDOT:PSS peaks at Week 0 (left) and Week 4 (right)

In Figure 35, the characteristic Raman vibrational modes for the PEDOT:PSS can be observed on both hydrogel A (PEDOT:PSS + TA) and hydrogel C (PEDOT:PSS + TA + CQD) at around 1000  $\text{cm}^{-1}$ , 1100  $\text{cm}^{-1}$ ,

1250  $\text{cm}^{-1}$ , 1360  $\text{cm}^{-1}$  and 1400  $\text{cm}^{-1}$ . The 1000  $\text{cm}^{-1}$  and the 1100  $\text{cm}^{-1}$  are associated with the vibrational modes of the PSS component, while the 1250  $\text{cm}^{-1}$ , 1360  $\text{cm}^{-1}$  and 1400  $\text{cm}^{-1}$  are related to the vibrational modes of the  $\text{C}_\alpha\text{-C}_\alpha$ ,  $\text{C}_\beta\text{-C}_\beta$  and  $\text{C}_\alpha\text{=C}_\beta$  of the PEDOT structure (understanding  $\text{C}_\alpha$  as carbon atoms bonded to a functional group, and  $\text{C}_\beta$  as carbon atoms next to the  $\text{C}_\alpha$ ). Hence, the presence of PEDOT:PSS can be confirmed [40], [41]. Also, in the week 4 Raman spectrum, the peaks at 1100  $\text{cm}^{-1}$  are no longer visible. These peaks, corresponding to the PSS component, may indicate the loss of the PSS component (a phase separation) from the PEDOT:PSS additive through the weeks. As it could be seen in some reviewed literature, PSS takes an important role on degradation effects of samples that presented it, as well as, a degradation of the PEDOT:PSS with the temperature [42]–[44].

For the Tannic Acid, the Raman characteristic vibrational peaks should be visible at 1600  $\text{cm}^{-1}$  and 1700  $\text{cm}^{-1}$  according to the reviewed literature [45]. However, these two peaks are not visible in the Raman data that was obtained experimentally. A hypothesis could be the low concentration of TA that is added to the hydrogels (0.4% of hydrogel weight).

With the CQDs a similar effect is shown. According to the literature reviewed two peaks at around 1350  $\text{cm}^{-1}$  and 1600  $\text{cm}^{-1}$  were expected in the Raman spectrum but none of them are visible [46], [47]. Again, as the concentration of CQDs in the hydrogels is so low (0.04% of hydrogel weight) the Raman peaks may not be appearing in the spectrums. Another hypothesis for the CQDs peaks not appearing could be the fluorescence behavior that they have. As Raman measures the transmittance of the samples, the fluorescence properties of CQDs may be suppressing the Raman signal. To confirm then the presence of CQDs on the solution, a visual inspection/test was performed, as it can be seen on Figure 33.

Finally, if the TA + CQD Raman spectrum is analyzed, it can be seen that no peaks are shown. Considering the low concentrations of TA and CQD on the hydrogels, what should be expected is, at least, find a peak at around 1400  $\text{cm}^{-1}$  from the PVA. A hypothesis for those peaks not showing is the interaction that PVA presents with the additives, causing its signal to not appear on the Raman spectrum. In the hydrogels that have PEDOT:PSS on it, the 1400  $\text{cm}^{-1}$  PVA peak is being overlaid by the PEDOT  $\text{C}_\alpha\text{=C}_\beta$  peak, that is the reason why a peak is appearing on that Raman shift. Also, the effect of the CQD fluorescence capacities could be altering/suppressing the PVA peak.

## 5.7. Final Data Analysis

In this final section of the project, a final analysis of all data obtained and previously analyzed is going to be discussed and correlated. To have a better look at the data obtained through the project, the following tables show the data obtained at degradation, swelling ration and pore size tests:

Table 5 Comparative table of Degradation, Swelling Ratio, SC and Pore Size of Week 0 samples

<b>Hydrogels</b>	<b>Degradation (%) Week 1</b>	<b>Swelling Ratio (%) Week 1</b>	<b>SC (mF/g) Week 0</b>	<b>Pore Size (<math>\mu\text{m}</math>) Week 0</b>
<b>A (PEDOT:PSS + TA)</b>	9,10 $\pm$ 7,57	737,45 $\pm$ 48,89	0,57 $\pm$ 0,09	3,49 $\pm$ 1,68
<b>B (TA + CQD)</b>	7,10 $\pm$ 0,29	575,01 $\pm$ 25,95	0,93 $\pm$ 0,08	2,32 $\pm$ 0,95
<b>C (PEDOT:PSS + TA + CQD)</b>	9,30 $\pm$ 0,30	816,81 $\pm$ 49,39	0,79 $\pm$ 0,07	2,75 $\pm$ 1,15
<b>D (PVA only)</b>	11,87 $\pm$ 4,16	391,50 $\pm$ 65,01	0,27 $\pm$ 0,02	2,09 $\pm$ 0,69

For the first table, as no pore size measurements were obtained from week 1 samples the comparison is done with the pore size values of the week 0 samples.

Table 6 Comparative table of Degradation, Swelling Ratio, SC and Pore Size values of Week 4 samples

<b>Hydrogels</b>	<b>Degradation (%) Week 4</b>	<b>Swelling Ratio (%) Week 4</b>	<b>SC (mF/g) Week 4</b>	<b>Pore Size (<math>\mu\text{m}</math>) Week 4</b>
<b>A (PEDOT:PSS + TA)</b>	23,50 $\pm$ 1,54	557,11 $\pm$ 27,12	0,12 $\pm$ 0,02	2,73 $\pm$ 1,03
<b>B (TA + CQD)</b>	25,94 $\pm$ 0,92	534,16 $\pm$ 28,69	0,19 $\pm$ 0,01	2,07 $\pm$ 0,68
<b>C (PEDOT:PSS + TA + CQD)</b>	31,40 $\pm$ 1,69	608,87 $\pm$ 32,51	0,16 $\pm$ 0,02	2,21 $\pm$ 0,80
<b>D (PVA only)</b>	17,31 $\pm$ 1,04	350,18 $\pm$ 26,93	0,11 $\pm$ 0,02	1,73 $\pm$ 0,41

With this data visible in the tables it is possible to observe much clearer the correlation between the different tests.

As it can be seen on both Table 5 and Table 6 a clear effect of the PEDOT:PSS additive on the hydrogels physical and chemical properties is shown, as both hydrogels that have this additive on their structure obtained the highest swelling ratio and the pore size through the weeks.

If the swelling and pore size data are analyzed together a relation between them can be observed as the bigger the pores on the hydrogels the higher the swelling. However, in some cases the number of pores (the pore size distribution (Figure 31)) produced a bigger effect on the swelling than the pore size itself. So, as it was already commented on the SEM section, the relation between pore volume/sample volume was the clear influence on the swelling ratio.

Another aspect that can be drawn by looking at the tables is the inversely proportional relationship between the degradation and the swelling ratio of the samples. As it can be seen, as the degradation values of the hydrogels increase the swelling ratios decrease, as the structure of the hydrogels is being affected and so the inner volume that can be filled is getting lower.

Following with the degradation data, analyzing all the tables, a clear degradation process is observed as the swelling ratio data and the pore size values decrease over the course of the 4 weeks. As it was explained in the previous paragraph, the structure is getting affected by the loss of additives and PVA itself. That way the pore structure is disrupted (resulting in a reduction on the pore size) and the inner volume of the sample able to be filled gets reduced. Also, a clear increase on the degradation values is shown.

Also, during the analysis it could be observed how the addition of the different additive really improved the physical and chemical characteristics of the hydrogel as, if the values in all tests are compared with the PVA only hydrogel (the blank), a clear improvement is observed. Also, an increase on degradation was suffered with the addition of all additives, being the hydrogel that degraded the most the one that includes all 3 studied additives on its structure.

If the conducting properties are now analyzed (CV and SC) it could also be seen how the addition of the additives produced an improvement on the electrochemical properties of the hydrogels compared to the PVA only hydrogel. Also, a relation between the loss of electroactivity and the degradation test

was observable as the current peaks and areas of CV and the SC were reduced through the weeks, following a similar trend as the degradation data.

Finally, the presence of the different additives could be confirmed with the FTIR and Raman data. Even though some additive peaks did not show on the spectrums (like TA and CQDs), their presence was confirmed by other tests (Figure 33). Also, through these two tests a degradation process was observable after comparing the data through the weeks.

## 6. Environmental Impact Analysis

To calculate the environmental impact of this project two concepts are going to be considerate: the kg of CO<sub>2</sub> produced by the equipment and laboratory used, and the material waste that cannot be reused.

For the electricity usage, the following table was obtained:

Table 7 Power consumption during the project and the equivalent kg of CO<sub>2</sub> produced considering a production of 250g of CO<sub>2</sub> per kW/h

<b>POWER CONSUMED</b>	<b>KW</b>	<b>HOURS OF USE</b>	<b>KWH</b>	<b>KG CO<sub>2</sub></b>
<b>LABORATORY LIGHTS (6 LED FLUORESCENT TUBES)</b>	0,12	1200	144	36
<b>HEATING PLATE</b>	1,5	70	105	26,25
<b>FREEZER -80°C</b>	1,75	2880	5040	1260
<b>FREEZER -20°C</b>	0,55	2880	1584	396
<b>FRIDGE 4°C</b>	0,4	2880	1152	288
<b>LYOPHILIZER</b>	1,1	480	528	132
<b>TOTAL KG CO<sub>2</sub> PRODUCED</b>				<b>2138,25</b>

For the kW the following considerations were took in mind:

- For the laboratory lights is was considered that the laboratory lights were on for 10h a day during the 4 months, making a total of 1200h.
- The freezers and fridge were considered to be working 24h a day during the 4 months of the project, making a total of 2880h.
- For the heating plate and the lyophilizer were considered to be working only when samples were placed drying samples or heating the hydrogel solutions.



As it can be seen on the table, a total of **2138,25 kg of CO<sub>2</sub>** were produced during this project just by the power consumption of essential equipment and laboratory light.

For the material waste a total of **7,90kg** of material was calculated during the project. This material waste includes Eppendorf tubes, Micropipette tips (considered a bag of 500 units), laboratory gloves and a 130m paper roll. It is important to have in consideration that this material that was considered are materials that could not be reused under any circumstances.

Good laboratory behaviors were used while doing the project in order to avoid the waste of material as well as to lower power consumption and water waste, for example working different samples on the same equipment to avoid dead times of power consumption, cleaning the maximum material at once to avoid water waste, reusing all possible laboratory material (tips, pipettes, Petri dishes, Falcon tubes, etc.).



## Budget and Economic Analysis

In this section, an economic evaluation of this project is presented. This evaluation was divided in two parts: materials and human costs. The budget then is presented in the next tables:

The economic calculus of the reagents is calculated by the amount of reagent used during the project. Knowing the total amount of reagent bought and the price, the expenses for the reagents used can be calculated as follows:

$$\text{Reagents cost (€)} = \frac{\text{reagent used (g)}}{\text{total reagent bought (g)}} * \text{price (€)}$$

Table 8 Total cost of the reagents used in the project

<b>REAGENTS</b>	<b>PRICE (€)</b>	<b>Mass or Volume of stock reagent</b>	<b>Reagent used</b>	<b>Price of reagents used (€)</b>
<b>PVA</b>	45,30	250g	12g	2,17
<b>PEDOT:PSS (0,65% wt)</b>	274,50	500g	25g	13,75
<b>Tannic Acid</b>	34,30	50g	0,92g	0,63
<b>Chitosan</b>	66,50	50g	1,2g	1,59
<b>NaCl</b>	23,50	500g	20g	0,94
<b>KCl</b>	84,70	1000g	0,5g	0,05
<b>Na<sub>2</sub>HPO<sub>4</sub></b>	92,40	500g	3,6g	0,67
<b>KH<sub>2</sub>PO<sub>4</sub></b>	57,50	500g	0,6g	0,07
<b>Acetic Acid</b>	232,76	2500ml	1,2ml	0,12
<b>TOTAL COST</b>				<b>19,99 €</b>

Table 9 Cost of the working ours based on a mean Junior Biomedical Engineer salary of 21.500€ a year [48]

<b>Total Hours (h)</b>	760
<b>Price per hour (€/h)</b>	8,25
<b>TOTAL COST</b>	<b>6270 €</b>

Table 10 Cost of project correction based on a mean Senior Engineer salary in Barcelona of 55.700€ a year [49]

<b>Total Hours (h)</b>	30
<b>Price per hour (€/h)</b>	17,5
<b>TOTAL COST</b>	<b>525 €</b>

Table 11 Total cost of the used equipment in the laboratory for the characterization. Prices are provided by the Barcelona Research Center in Multiscale Science and Engineering

<b>Equipment</b>	<b>Price per hour (€)</b>	<b>Hours</b>	<b>Price of usage (€)</b>
<b>FTIR</b>	22,5	4	90
<b>Focused Ion Beam SEM</b>	187,5	5	937,5
<b>Desktop SEM</b>	45	10	450
<b>RAMAN</b>	56,25	4	225
		<b>TOTAL COST</b>	<b>1702,5 €</b>

Table 12 Cost of the laboratory equipment used to perform the test based on their lifespan and time of use

<b>Equipment</b>	<b>Price (€)</b>	<b>Lifespan (Years)</b>	<b>Usage time (h)</b>	<b>Usage cost (€)</b>
<b>Potentiostat</b>	7900	10	100	9,01
<b>Lyophilizer</b>	5500	10	480	30,12
<b>TOTAL COST</b>				<b>39,13</b>

To calculate the costs of the lyophilizer and potentiostat usage, it was calculated in function of the lifespan of the equipment compared to the hours that was used. Then, the cost per usage of the equipment was calculated as follows:

$$\text{Cost per usage} = \frac{\text{Usage Time (h)}}{\text{Lifespan (h)}} * \text{Equipment price (€)}$$

Then, the total cost of this project that includes reagents, the use of the equipment and the working ours makes a total of **8556,62 €**

## Conclusions

This TFG shows the various steps followed to obtain PVA hydrogels with the presence of TA, CQD and PEDOT:PSS additives. Through the freeze-thawing method (and therefore without the presence of a crosslinking agent) all the hydrogels necessary for the different characterization tests established at the beginning, were synthesized. Therefore, the first of the objectives can be considered satisfactorily achieved.

Once all the data from the various tests have been analyzed and correlated with each other, the following conclusions can be drawn:

Regarding the electrochemical properties of the hydrogels, a clear improvement can be observed with the addition of the various additives. In the CV tests, it was observed that the hydrogel with the three additives present, showed the highest current peak of all. On the other hand, in the SC test, it was also possible to observe a clear improvement in the capacity of the hydrogels with the addition of the different additives.

Moving on to the degradation test, it was also possible to observe a clear increase in degradation with the addition of the additives where, once again, the hydrogel with the three of them present, obtained the highest value. At the same time, the degradation of the samples was much more pronounced during the first week, finding a small "stabilization" from the second. During the first week of the test, it was also possible to observe certain differences in the rate of degradation, as some samples found this "stabilization" at different time points.

Through various characterization tests, it has also been possible to observe relationships between the various tests. One of these has been the direct relationship observed in the analysis of the images obtained using the SEM technique. It has been observed that the samples that present a higher ratio  $(\text{pore volume})/(\text{sample volume})$  are those that have obtained a greater degradation and swelling values. Thanks to the data obtained with the FTIR technique and the visual observations made throughout the test, it was also possible to see a clear influence of the release of TA on the degradation.

In general conclusions, it has been observed that the addition of the different additives has led to an improvement in the electrochemical and physical properties of our samples. At the same time,

however, it has also induced an increase in the degradation of these. This feature could be used in some other experiments to try, for example, to tailor and/or enhance the degradation of hydrogels.

It has also been possible to observe the individual behavior of each of the components present in the hydrogels as well as the interaction that these have with each other, and how these processes affect the characteristics of the hydrogels.

Even so, the data in some tests has not been entirely consistent with what should be expected. That is why the points to be improved in this project would be the need to repeat some tests under much more established and maintained conditions for all the samples (both synthesis and procedure). Also, due to the time limitation for the realization of this TFG, it has been necessary to cut down on some aspects such as, for example, the number of samples of each hydrogel to be tested at each instant of time, or the number of tests done per technique.

## Bibliography

- [1] M. Chanda, "Introduction to Polymer Science and Chemistry", 2nd Edition. Boca Raton: CRC Press, 2013. doi: 10.1201/b14577.
- [2] R. O. Ebewele, "Polymer Science and Technology", 1st Edition. Boca Raton: CRC Press LLC, 2000.
- [3] F. W. Billmeyer, "Textbook of Polymer Science", 2nd Edition., vol. 10. New York: John Wiley & Sons, Inc., 1971. doi: 10.1002/pol.1972.110100721.
- [4] P. Goswami and T. O'Haire, "3 - Developments in the use of green (biodegradable), recycled and biopolymer materials in technical nonwovens", in *Advances in Technical Nonwovens*, G. Kellie, Ed. Woodhead Publishing, 2016, pp. 97–114. doi: <https://doi.org/10.1016/B978-0-08-100575-0.00003-6>.
- [5] C. Bastioli, Ed., "Handbook of Biodegradable Polymers", 3rd ed. De Gruyter, 2020. doi: 10.1515/9781501511967.
- [6] W. Amass, A. Amass, and B. Tighe, "A review of biodegradable polymers: uses, current developments in the synthesis and characterization of biodegradable polyesters, blends of biodegradable polymers and recent advances in biodegradation studies", *Polymer International*, vol. 47, no. 2, pp. 89–144, Oct. 1998, doi: 10.1002/(SICI)1097-0126(199810)47:2<89::AID-PI86>3.0.CO;2-F.
- [7] H. Adelnia, R. Ensandoost, S. Shebbrin Moonshi, J. N. Gavvani, E. I. Vasafi, and H. T. Ta, "Freeze/thawed polyvinyl alcohol hydrogels: Present, past and future", *European Polymer Journal*, vol. 164, p. 110974, 2022, doi: <https://doi.org/10.1016/j.eurpolymj.2021.110974>.
- [8] L. Majewski, "Alternative Gate Insulators for Organic Field-Effect Transistors", Jan. 2015. doi: 10.13140/2.1.3418.1929.
- [9] G. Inzelt, "Conducting Polymers", Berlin, Heidelberg: Springer Berlin Heidelberg, 2012. doi: 10.1007/978-3-642-27621-7.
- [10] T. Nezakati, A. Seifalian, A. Tan, and A. M. Seifalian, "Conductive Polymers: Opportunities and Challenges in Biomedical Applications", *Chemical Reviews*, vol. 118, no. 14, pp. 6766–6843, Jul. 2018, doi: 10.1021/acs.chemrev.6b00275.
- [11] L. Bolaños and L. Alvarez, "Polímeros conductores: aplicaciones en celdas fotovoltaicas y dispositivos electrónicos", pp. 18–38, Nov. 2019.



- [12] “The concept of ‘doping’ of conducting polymers: the role of reduction potentials”, *Philosophical Transactions of the Royal Society of London. Series A, Mathematical and Physical Sciences*, vol. 314, no. 1528, pp. 3–15, May 1985, doi: 10.1098/rsta.1985.0004.
- [13] A. B. S. Elliott, R. Horvath, and K. C. Gordon, “Vibrational spectroscopy as a probe of molecule-based devices”, *Chemical Society Reviews*, vol. 41, no. 5, pp. 1929–1946, 2012, doi: 10.1039/C1CS15208D.
- [14] G. Heywang and F. Jonas, “Poly(alkylenedioxythiophene)s—new, very stable conducting polymers”, *Advanced Materials*, vol. 4, no. 2, pp. 116–118, 1992, doi: <https://doi.org/10.1002/adma.19920040213>.
- [15] K. Sun *et al.*, “Review on application of PEDOTs and PEDOT:PSS in energy conversion and storage devices”, *Journal of Materials Science: Materials in Electronics*, vol. 26, pp. 1–25, Nov. 2015, doi: 10.1007/s10854-015-2895-5.
- [16] Q. Liu, J. Qiu, C. Yang, L. Zang, G. Zhang, and E. Sakai, “High-Performance PVA/PEDOT:PSS Hydrogel Electrode for All-Gel-State Flexible Supercapacitors”, *Advanced Materials Technologies*, vol. 6, no. 1, p. 2000919, 2021, doi: <https://doi.org/10.1002/admt.202000919>.
- [17] W. Cai, R. B. Gupta, and U. by Staff, “Hydrogels”, in *Kirk-Othmer Encyclopedia of Chemical Technology*, John Wiley & Sons, Ltd, 2012, pp. 1–20. doi: <https://doi.org/10.1002/0471238961.0825041807211620.a01.pub2>.
- [18] M. Negrato, “Electrochemical properties of carbon dots and their use as photocatalysts in c–o bond fragmentation”, Università Ca’ Foscari Venezia, Venezia, 2013.
- [19] Y. Wang and A. Hu, “Carbon quantum dots: synthesis, properties and applications”, *Journal of Materials Chemistry C*, vol. 2, no. 34, pp. 6921–6939, 2014, doi: 10.1039/C4TC00988F.
- [20] B. Wang and S. Lu, “The light of carbon dots: From mechanism to applications”, *Matter*, vol. 5, no. 1, pp. 110–149, 2022, doi: <https://doi.org/10.1016/j.matt.2021.10.016>.
- [21] S. Campuzano, P. Yáñez-Sedeño, and J. M. Pingarrón, “Carbon Dots and Graphene Quantum Dots in Electrochemical Biosensing”, *Nanomaterials*, vol. 9, no. 4, p. 634, Apr. 2019, doi: 10.3390/nano9040634.
- [22] X. Wang, Y. Feng, P. Dong, and J. Huang, “A Mini Review on Carbon Quantum Dots: Preparation, Properties, and Electrocatalytic Application”, *Frontiers in Chemistry*, vol. 7, Oct. 2019, doi: 10.3389/fchem.2019.00671.

- [23] S. H. Omar, "Chapter 4 - Biophenols: Impacts and Prospects in Anti-Alzheimer Drug Discovery", in *Discovery and Development of Neuroprotective Agents from Natural Products*, G. Brahmachari, Ed. Elsevier, 2018, pp. 103–148. doi: <https://doi.org/10.1016/B978-0-12-809593-5.00004-5>.
- [24] H. Fan, J. Wang, Q. Zhang, and Z. Jin, "Tannic Acid-Based Multifunctional Hydrogels with Facile Adjustable Adhesion and Cohesion Contributed by Polyphenol Supramolecular Chemistry", *ACS Omega*, vol. 2, no. 10, pp. 6668–6676, 2017, doi: [10.1021/acsomega.7b01067](https://doi.org/10.1021/acsomega.7b01067).
- [25] N. Elgrishi, K. J. Rountree, B. D. McCarthy, E. S. Rountree, T. T. Eisenhart, and J. L. Dempsey, "A Practical Beginner's Guide to Cyclic Voltammetry", *Journal of Chemical Education*, vol. 95, no. 2, pp. 197–206, Feb. 2018, doi: [10.1021/acs.jchemed.7b00361](https://doi.org/10.1021/acs.jchemed.7b00361).
- [26] O. J. Guy and K.-A. D. Walker, "Graphene Functionalization for Biosensor Applications", in *Silicon Carbide Biotechnology*, 2nd Edition., S. E. Saddow, Ed. Elsevier, 2016, pp. 85–141. doi: [10.1016/B978-0-12-802993-0.00004-6](https://doi.org/10.1016/B978-0-12-802993-0.00004-6).
- [27] J. Heinze, "Cyclic Voltammetry 'Electrochemical Spectroscopy'. New Analytical Methods", *Angewandte Chemie International Edition in English*, vol. 23, no. 11, pp. 831–847, 1984, doi: <https://doi.org/10.1002/anie.198408313>.
- [28] D. J. Stokes, "Principles and Practice of Variable Pressure/Environmental Scanning Electron Microscopy (VP-ESEM)", Wiley, 2008. doi: [10.1002/9780470758731](https://doi.org/10.1002/9780470758731).
- [29] M. Cubells Pérez, "Análisis de pigmentos con espectroscopía Raman: determinación teórico-experimental de la temperatura inducida por el láser", Universitat Politècnica de Catalunya, Barcelona, 2013.
- [30] P. R. Griffiths and J. A. de Haseth, "Fourier Transform Infrared Spectrometry", Hoboken, NJ, USA: John Wiley & Sons, Inc., 2007. doi: [10.1002/047010631X](https://doi.org/10.1002/047010631X).
- [31] B. Wang *et al.*, "Construction and Electrochemical Properties of Solid-state Supercapacitors with Redox Additives", *Chemistry – An Asian Journal*, vol. 17, no. 18, p. e202200702, 2022, doi: <https://doi.org/10.1002/asia.202200702>.
- [32] X. Sun, H. Wang, J. Qi, S. Zhou, and H. Li, "Supramolecular self-assemblies formed by co-assembly of carbon dots and tannic acid", *Dyes and Pigments*, vol. 190, p. 109287, 2021, doi: <https://doi.org/10.1016/j.dyepig.2021.109287>.
- [33] I. Jipa *et al.*, "Potassium sorbate release from poly(vinyl alcohol)-bacterial cellulose films", *Chemical Papers*, vol. 66, no. 2, Jan. 2012, doi: [10.2478/s11696-011-0068-4](https://doi.org/10.2478/s11696-011-0068-4).

- [34] S.-S. Chang, L. Salmén, A.-M. Olsson, and B. Clair, "Deposition and organisation of cell wall polymers during maturation of poplar tension wood by FTIR microspectroscopy", *Planta*, vol. 239, no. 1, pp. 243–254, Jan. 2014, doi: 10.1007/s00425-013-1980-3.
- [35] K. H. Hong, "Polyvinyl alcohol/tannic acid hydrogel prepared by a freeze-thawing process for wound dressing applications", *Polymer Bulletin*, vol. 74, no. 7, pp. 2861–2872, Jul. 2017, doi: 10.1007/s00289-016-1868-z.
- [36] X. Wang, M. Li, G. Feng, and M. Ge, "On the mechanism of conductivity enhancement in PEDOT:PSS/PVA blend fiber induced by UV-light irradiation", *Applied Physics A*, vol. 126, no. 3, p. 184, Mar. 2020, doi: 10.1007/s00339-019-3271-8.
- [37] V. Hebbbar, R. F. Bhajantri, and J. Naik, "Influence of graphene nanoparticles on optical and dielectric properties of PVA-PEDOT:PSS blend composite", 2017, p. 050046. doi: 10.1063/1.4980279.
- [38] Z. Zhang, T. Li, B. Chen, S. Wang, and Z. Guo, "Self-healing supramolecular hydrogel of poly(vinyl alcohol)/chitosan carbon dots", *Journal of Materials Science*, vol. 52, no. 17, pp. 10614–10623, Sep. 2017, doi: 10.1007/s10853-017-1222-3.
- [39] Y. Shi, D. Xiong, J. Li, K. Wang, and N. Wang, "In situ repair of graphene defects and enhancement of its reinforcement effect in polyvinyl alcohol hydrogels", *RSC Advances*, vol. 7, no. 2, pp. 1045–1055, 2017, doi: 10.1039/C6RA24949C.
- [40] S. Chang, C.-H. Chiang, F. S. Kao, C.-L. Tien, and C.-G. Wu, "Unraveling the Enhanced Electrical Conductivity of PEDOT:PSS Thin Films for ITO-Free Organic Photovoltaics", *IEEE Photonics J*, vol. 6, p. 8400307, Jan. 2014.
- [41] T. A. Yemata *et al.*, "Modulation of the doping level of PEDOT:PSS film by treatment with hydrazine to improve the Seebeck coefficient", *RSC Advances*, vol. 10, no. 3, pp. 1786–1792, 2020, doi: 10.1039/C9RA07648D.
- [42] E. Vitoratos, S. Sakkopoulos, N. Paliatsas, K. Emmanouil, and S. A. Choulis, "Conductivity Degradation Study of PEDOT: PSS Films under Heat Treatment in Helium and Atmospheric Air", *Open Journal of Organic Polymer Materials*, vol. 02, no. 01, pp. 7–11, 2012, doi: 10.4236/ojopm.2012.21002.
- [43] Y. Shi *et al.*, "Degradation phenomena and degradation mechanisms for highly conductive PEDOT:PSS films", *Materials Letters*, vol. 308, p. 131106, 2022, doi: <https://doi.org/10.1016/j.matlet.2021.131106>.
- [44] E. Vitoratos *et al.*, "Thermal degradation mechanisms of PEDOT:PSS", *Organic Electronics*, vol. 10, no. 1, pp. 61–66, 2009, doi: <https://doi.org/10.1016/j.orgel.2008.10.008>.

- [45] D. R. Pompeu, Y. Larondelle, H. Rogez, O. Abbas, J. A. F. Pierna, and V. Baeten, “Characterization and discrimination of phenolic compounds using Fourier transform Raman spectroscopy and chemometric tools”, *BASE*, pp. 13–28, Oct. 2018, doi: 10.25518/1780-4507.16270.
- [46] A. Dager, A. Baliyan, S. Kurosu, T. Maekawa, and M. Tachibana, “Ultrafast synthesis of carbon quantum dots from fenugreek seeds using microwave plasma enhanced decomposition: application of C-QDs to grow fluorescent protein crystals”, *Science Report*, vol. 10, no. 1, p. 12333, 2020, doi: 10.1038/s41598-020-69264-9.
- [47] X. Ma, S. Li, V. Hessel, L. Lin, S. Meskers, and F. Gallucci, “Synthesis of luminescent carbon quantum dots by microplasma process”, *Chemical Engineering and Processing - Process Intensification*, vol. 140, pp. 29–35, 2019, doi: <https://doi.org/10.1016/j.cep.2019.04.017>.
- [48] Glassdoor, Inc., “How much does a Junior Engineer make in Barcelona, Spain?”, *Junior Engineer Salaries*, Last update: January 13, 2023, Accessed: January 4, 2023, Available at: [https://www.glassdoor.com/Salaries/barcelona-junior-engineer-salary-SRCH\\_IL.0,9\\_IM1015\\_KO10,25.htm](https://www.glassdoor.com/Salaries/barcelona-junior-engineer-salary-SRCH_IL.0,9_IM1015_KO10,25.htm)
- [49] Glassdoor, Inc., “How much does a Senior Engineer make in Barcelona, Spain?”, *Senior Engineer Salaries*, Last update: January 13, 2023, Accessed: January 4, 2023, Available at: [https://www.glassdoor.com/Salaries/barcelona-senior-engineer-salary-SRCH\\_IL.0,9\\_IM1015\\_KO10,25.htm](https://www.glassdoor.com/Salaries/barcelona-senior-engineer-salary-SRCH_IL.0,9_IM1015_KO10,25.htm)

## Annexes

In this section, some plots of the single component hydrogels and data that was not essential during the analysis are shown, in order to cite them while analyzing if needed.

### A1. Cyclic Voltammetry

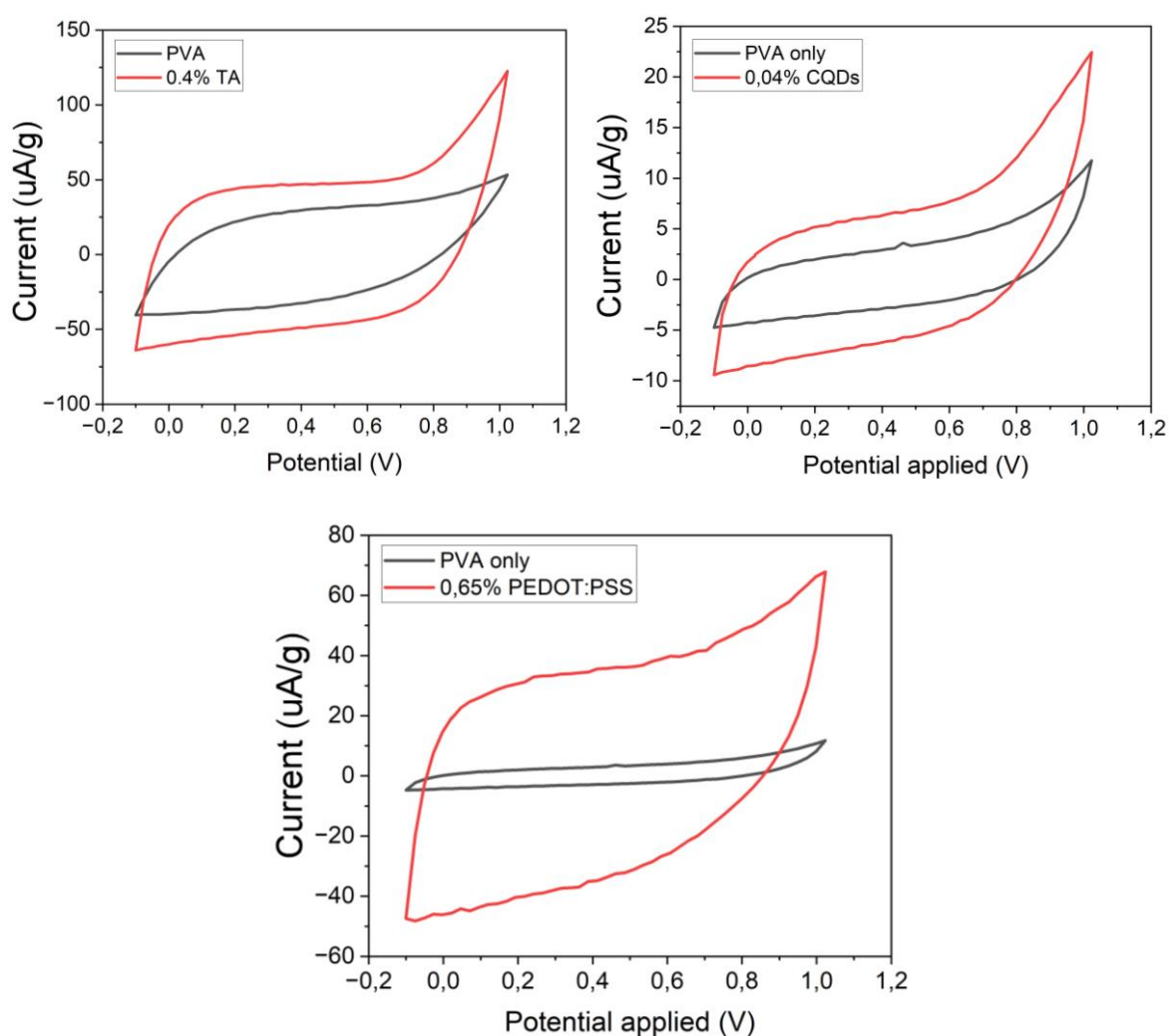


Figure 36 Single Component hydrogels CV compared with the PVA only

## A2. Degradation

### Single Component 1 Week degradation test

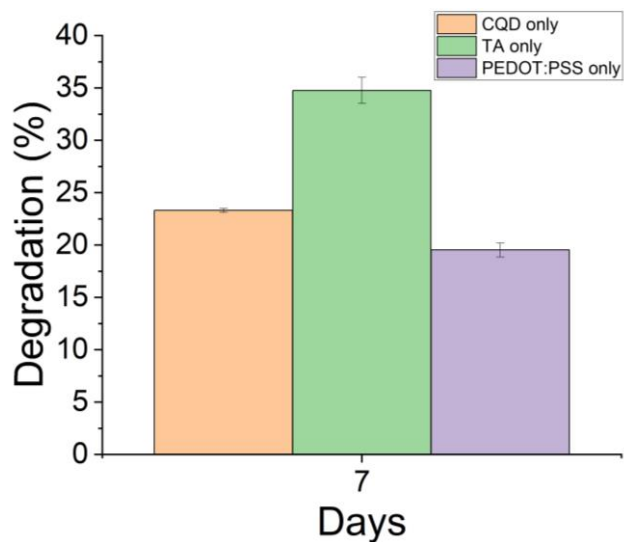


Figure 37 Day 7 degradation of single component hydrogels after 1 week test

## A3. Swelling Ratio

### Single component hydrogels 1 week swelling ratio test

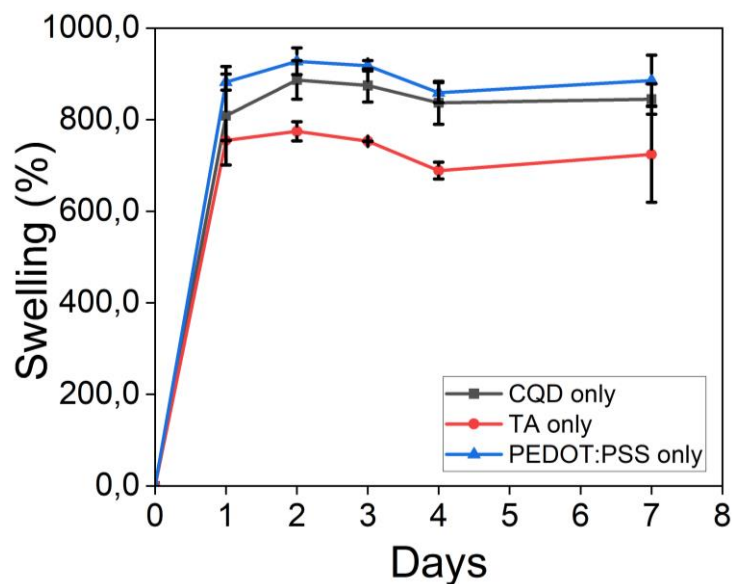


Figure 38 1 Week Swelling ratio test of single component hydrogels

## A4. SEM

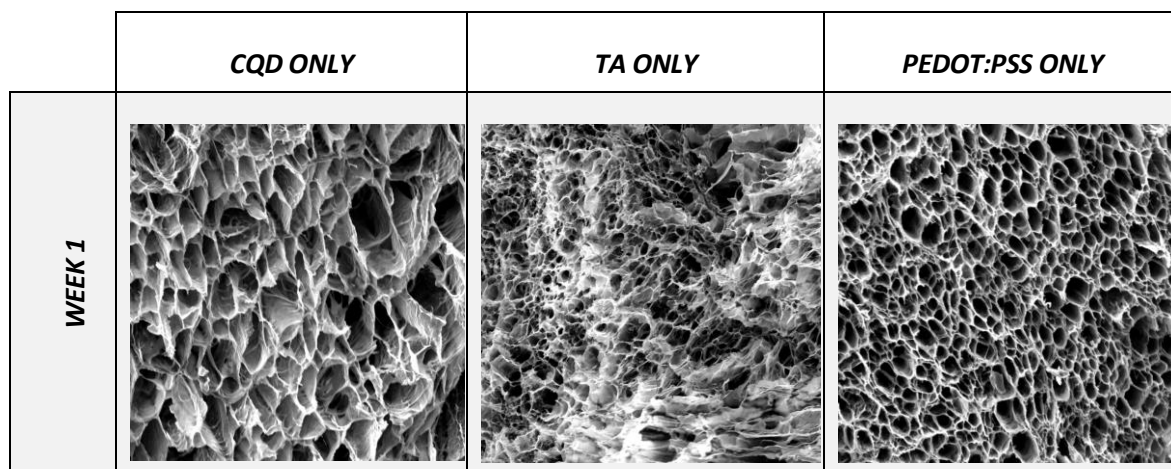


Figure 39 Visual comparison of single component hydrogels cross section

### Histograms

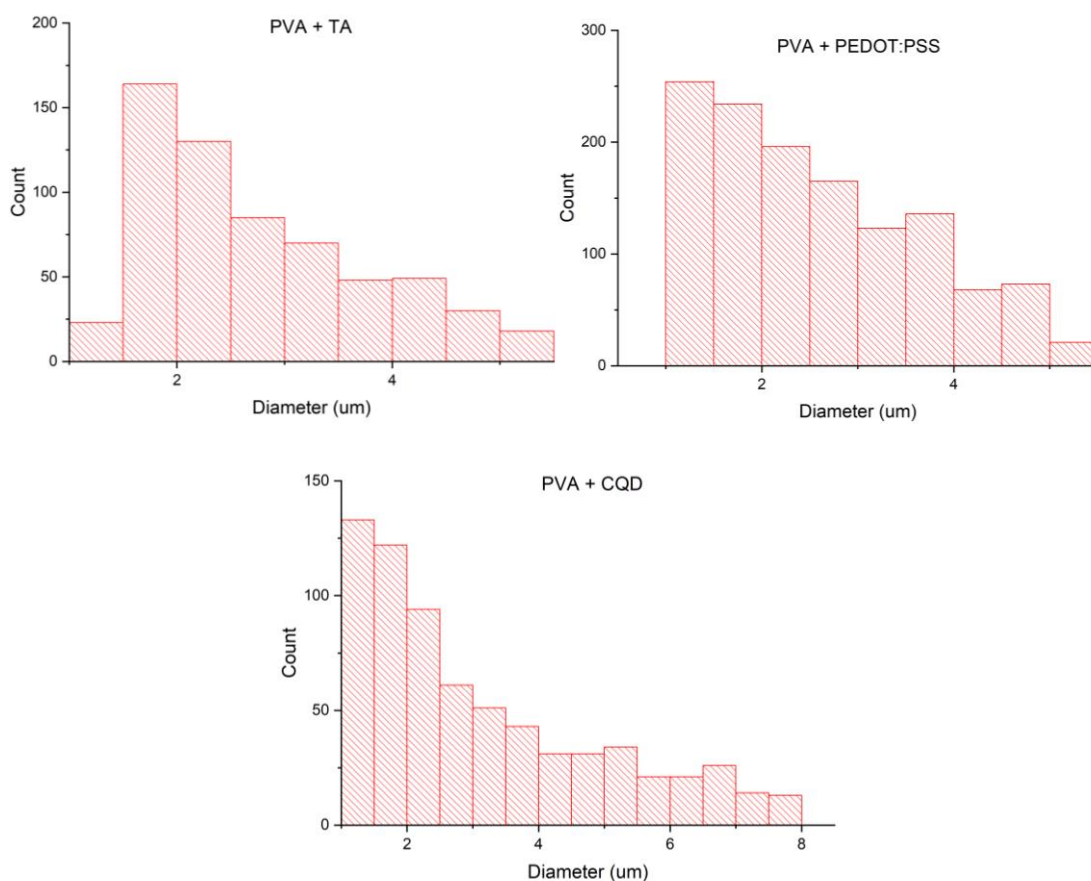


Figure 40 Single component hydrogels pore size histograms on week 0

## A5. FTIR

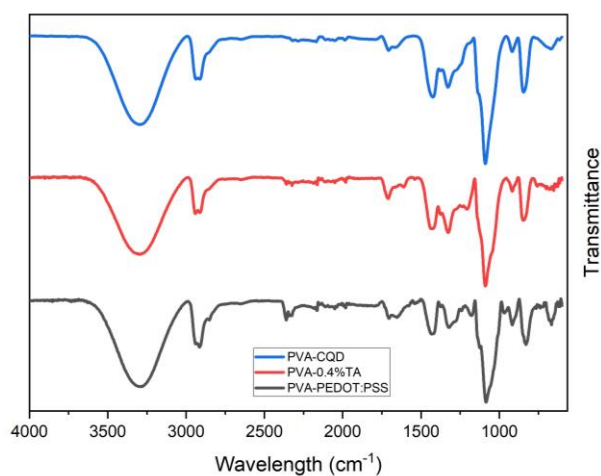


Figure 41 FTIR spectrums of the single component hydrogels on week 0

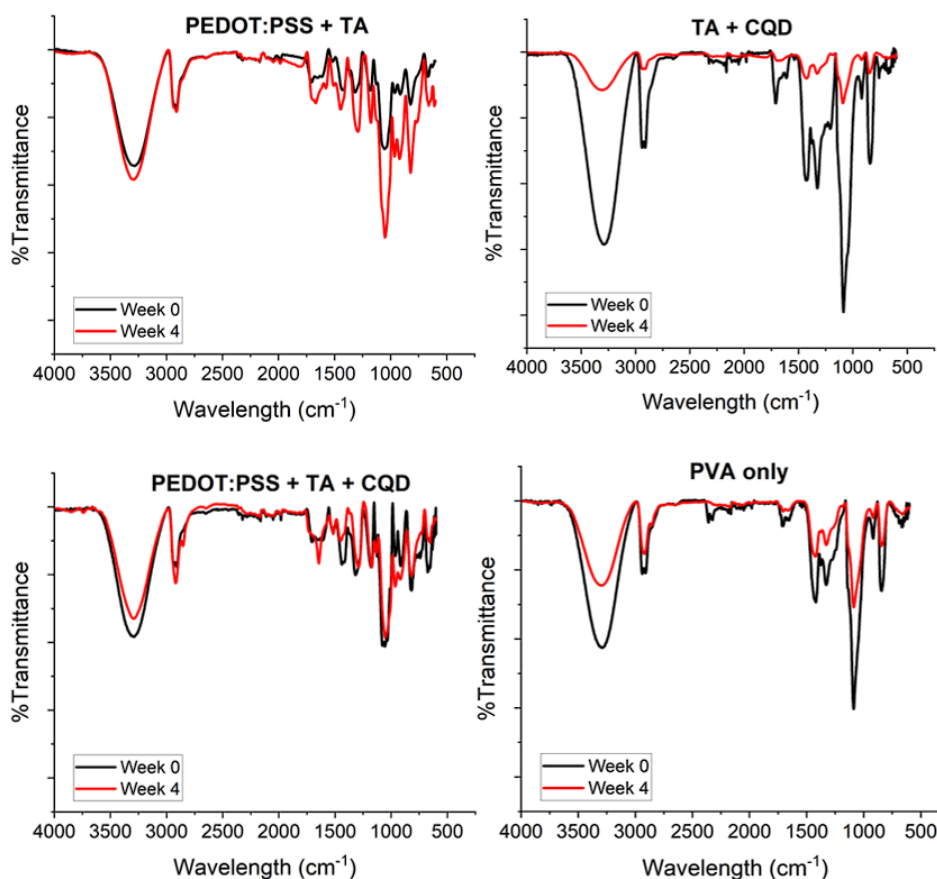


Figure 42 Comparison of FTIR spectrums on Week 0 and Week 4 of all hybrid hydrogels